Journal of Theoretical Biology 380 (2015) 569–584

Contents lists available at ScienceDirect

Journal of Theoretical Biology

journal homepage: www.elsevier.com/locate/yjtbi

A model for effects of adaptive immunity on tumor response to chemotherapy and chemoimmunotherapy

Mark Robertson-Tessi [a,d,*], Ardith El-Kareh [b], Alain Goriely [c]

[a] Program in Applied Mathematics, University of Arizona, Tucson, AZ 85721, United States
[b] ARL-Microcirculation Division, University of Arizona, Tucson, AZ 85724, United States
[c] Mathematical Institute, University of Oxford, Woodstock Road, OX2 6GG, UK
[d] Integrated Mathematical Oncology, Moffitt Cancer Center, Tampa, FL 33612, United States

HIGHLIGHTS

- We model the effect of the adaptive immune system during therapy.
- The immune system may contribute to tumor cure and extended survival.
- Combination chemoimmunotherapies have potential synergy, for tumors with certain properties.

ARTICLE INFO

Article history:
Received 29 October 2013
Received in revised form
8 May 2015
Accepted 2 June 2015
Available online 16 June 2015

Keywords:
Mathematical model
Tumor immunology
Treatment optimization

ABSTRACT

Complete clinical regressions of solid tumors in response to chemotherapy are difficult to explain by direct cytotoxicity alone, because of low growth fractions and obstacles to drug delivery. A plausible indirect mechanism that might reconcile this is the action of the immune system. A model for interaction between tumors and the adaptive immune system is presented here, and used to examine controllability of tumors through the interplay of cytotoxic, cytostatic and immunogenic effects of chemotherapy and the adaptive immune response. The model includes cytotoxic and helper T cells, T regulatory cells (Tregs), dendritic cells, memory cells, and several key cytokines. Nearly all parameter estimates are derived from experimental and clinical data. Individual tumors are characterized by two parameters: growth rate and antigenicity, and regions of tumor control are identified in this parameter space. The model predicts that inclusion of the immune response significantly expands the region of tumor control for both cytostatic and cytotoxic chemotherapies. Moreover, outside the control zone, tumor growth is delayed significantly. An optimal fractionation schedule is predicted, for a fixed cumulative dose. The model further predicts expanded regions of tumor control when several forms of immunotherapy (adoptive T cell transfer, Treg depletion, and dendritic cell vaccination) are combined with chemotherapy. Outcomes depend greatly on tumor characteristics, the schedule of administration, and the type of immunotherapy chosen, suggesting promising opportunities for personalized medicine. Overall, the model provides insight into the role of the adaptive immune system in chemotherapy, and how scheduling and immunotherapeutic interventions might improve efficacy.

1. Introduction and motivation

Complete clinical regressions of tumors in response to chemotherapy are seen in a small percentage of patients (Wiltshaw, 1979; Bosl et al., 1983; Laino, 2013). It is difficult to explain this through direct drug-induced cell killing alone, for several reasons. First, it is widely believed that only proliferating cells respond to most chemotherapeutic agents (Carlisle et al., 2002; Kerbel and Kamen, 2004; Gerber, 2008), yet much evidence suggests that only a small fraction of the cells in a tumor are actively proliferating at any point in time (Tay et al., 1991; McKinnell, 1998). Second, significant transport obstacles, caused by highly irregular vascular structure (Pries et al., 2009) and the tumor microenvironment, make homogeneous delivery of drugs to all cells of a tumor virtually impossible (Minchinton and Tannock, 2006; Trédan et al., 2007). This gap in our understanding of how chemotherapy actually works (when it does) has led investigators to search for other indirect mechanisms by which chemotherapy might lead to large-scale tumor regression (Goodman, 2004; Vo et al., 2012). While several mechanisms could be proposed, including bystander

* Corresponding author.
E-mail address: mark.robertsontessi@moffitt.org (M. Robertson-Tessi).

http://dx.doi.org/10.1016/j.jtbi.2015.06.009
0022-5193/

effects from cell–cell signaling (Jensen and Glazer, 2004) and the stem cell theory of cancer (which holds that only a fraction of the cells in a tumor are clonogenic and therefore only this fraction must be killed) (Gong et al., 2011), a likely candidate appears to be the interaction of the immune system with the tumor (Manthey et al., 1994; Goodman, 2004; Newell et al., 2004).

Among the pieces of compelling evidence supporting the idea that immune effects play an important role in chemotherapy is the study of McCoy et al. (2012) which found that the change in $CD8^+$ T cell proliferation fraction after a single cycle of chemotherapy was predictive of outcome. McCoy et al. also observed that mice with a defective T-cell compartment did not respond well to chemotherapy.

Our previous study (Robertson-Tessi et al., 2012) examined the dynamic interplay between the adaptive immune system and the tumor, including its regulatory components, and found that an optimal range of antigenicity existed for tumor control: counter-intuitively, increasing antigenicity was not always beneficial. Interestingly, such a conclusion could not be reached by considering cellular-level interactions alone, as it relies on the nonlinear evolution of the system. In the present study, we use this framework of integrated dynamic simulations to examine the interactions between the tumor and the adaptive immune system in the context of chemotherapy and chemoimmunotherapy.

That chemotherapy has immunostimulatory effects is a fact that was underappreciated until the last decade; previously, chemotherapy was widely viewed as having only immunosuppressive effects. More recently, a number of different ways in which chemotherapy may enhance the anti-tumor immune response have been investigated. Direct cell kill by apoptosis may increase antigen presentation (Pfannenstiel et al., 2010). Paclitaxel was found to enhance dendritic cell activation (Pfannenstiel et al., 2010). Chemotherapy may also increase the anti-tumor effect of T cells (Bergmann-Leitner and Abrams, 2001; Baxevanis et al., 2009). It can alter the tumor microenvironment, making it easier for immune cells to gain access to the tumor. Even the T-cell depletion resulting from chemotherapy may, perhaps counterintuitively, be beneficial, by either eliminating immune components (such as regulatory T cells) that are responsible for immunosuppression, or by creating an opportunity space for homeostatic proliferation of tumor-specific cytotoxic T cells (Baxevanis et al., 2009).

Immunostimulation by chemotherapy has mostly been studied at the cellular level. However, cellular-level effects occur in conjunction with the simultaneous and interwoven kinetic processes of tumor regression, regrowth, and the dynamics of the immune system. The net results of these time-evolving interactions cannot necessarily be understood by considering cellular-level modulations in isolation. At first glance, chemotherapy appears to have only a short-term effect on several components of the adaptive immune system, such as a significant reduction in size of the regulatory T-cell (Treg) population (Ercolini et al., 2005; Lutsiak et al., 2005), which subsequently recovers. Yet these temporary effects of chemotherapy on the adaptive immune system might translate into a longer-term effect on tumor control by essentially resetting the tumor to a different initial state. Thus, chemotherapy may act synergistically with the immune system in a way that explains why either long-term control or delay of relapse can occur even when direct drug-induced kill is possible only for a fraction of the tumor cells. Even the additional consideration of cellular-level effects such as post-chemotherapy enhanced lytic ability of effector cells (Bergmann-Leitner and Abrams, 2001) may not suffice to explain the total resultant. The present model examines this potentially important possibility by simulating the dynamic interplay between the adaptive immune system and clinically detectable tumors treated by chemotherapy. A novel feature in the immune component of our model is the inclusion of the conversion of helper T cells into Treg cells, which may be a significant source of Treg cells and thus immunosuppression (Liu et al., 2007), particularly in late-stage tumors. Also, our previous study found that treating helper cells as a distinct population was essential for obtaining physiologically reasonable T-cell dynamics; thus, this approach is retained in the present model. While many cellular-level immunostimulatory effects of chemotherapy could be included, the present model focuses on the enhancement of effector cell-induced tumor cell lysis by chemotherapeutic drugs, as found by Bergmann-Leitner and Abrams (2001); other effects are left for future studies. In addition to addressing the question of whether immune effects partially explain chemotherapy response, the model is also used to investigate what immune interventions might possibly enhance the effect of chemotherapy.

A number of previous studies have presented mathematical models for tumor–immune interactions and their effect on tumor growth and treatment response. Some have focused on the adaptive immune system, as is done in the present study, while others have been concerned with the innate immune system. Most of these models involve deterministic systems of ordinary differential equations (Kirschner and Panetta, 1998; de Pillis et al., 2005), an approach adopted here as well. However, some studies have employed stochastic differential equations, to capture natural fluctuations in immune levels. Notable among such studies are Caravagna et al. (2010), d'Onofrio (2010), and d'Onofrio and Ciancio (2011); these works showed that stochastic effects can have a significant influence on tumor control.

Experimental studies also point to changes in tumor–immune interaction parameters over time, which may be due to emergence of certain immunoresistant tumor clones under selection pressure by the immune system (Matsushita et al., 2012), or to changes in antigen expression of the tumor cells in the absence of clonal selection or mutation (Bubeník, 2004), or to tumor-induced changes in the immune system itself (Reiman et al., 2007). The term "immunoediting" (Reiman et al., 2007) has been variously applied to all such forms of evolution, albeit without a consensus yet on its precise definition. Mathematical models have been developed to capture the effects of such time-evolution processes (d'Onofrio and Ciancio, 2011; Al-Tameemi et al., 2012). However, in the present study, with the goal of an initial exploration of the interplay between the tumor, chemotherapy/chemoimmunotherapy, immunosuppression effects, and the various subpopulations of the adaptive immune system, a simpler modeling approach was adopted wherein tumor–immune interactions are described deterministically with parameters assumed static over time.

2. Equations

The modeling of chemotherapeutic treatment without any consideration of immune effects is a rich field of its own. Despite the fact that the exact mechanism by which chemotherapy works is not completely understood, many models have been developed to explain the delivery and effect of the drugs involved (Sanga et al., 2006). In this paper, the specific cellular mechanisms of action of the drug are not modeled; rather, the model incorporates chemotherapy either as a dynamical change in the populations of tumor and T cells over short time periods, or as a cytostatic effect (Schmitt, 2007), whereby the tumor cells are prevented from reproducing for a short time period, after which they resume normal growth. Combination chemotherapy can include both cytotoxic and cytostatic drugs.

The present model is built on our previous model of tumor–immune interactions (Robertson-Tessi et al., 2012), with additional terms for the effects of chemotherapy. The model incorporates tumor cells (T), unlicensed (U) and licensed (D) dendritic cells (Abbas et al., 2012; Palucka and Banchereau, 2012), and three

types of T cells (effector T cells (E), helper T cells (H), and regulatory T cells (R)) (Abbas et al., 2012; Josefowicz et al., 2012), which exist in three states (memory cells (M_X), activated cells (A_X), and mature cells (X), where X represents any of the three types of T cells). Table 1 summarizes these state variables. Effector cells and regulatory T cells are populations in the tumor; all other immune cell subpopulations are in the lymph node compartment. There are three molecules in the model: the two interleukins IL-2 (C) and IL-10 (I), and TGF-β (S) (Abbas et al., 2012). These variables represent concentrations in the tumor and associated lymphatic periphery, which is assumed to be in equilibrium with the tumor.

The following equations are used to model the tumor–immune interactions:

$$\dot{T_g} = \frac{T_g}{\left(\left(\frac{1}{\gamma_1}\right)^p + \left(\frac{T_g^{1-m}}{\gamma}\right)^p\right)^{1/p}} - \frac{r(1-f_T)r_0 T^*}{\left(1+k_2\frac{T^*}{E}\right)} \times \frac{1}{\left(1+k_3\frac{R}{E}\right)\left(1+\frac{S}{S_1}\right)} \tag{2.1}$$

$$\dot{T_c} = -\frac{\ln(T_{c,0})}{\tau_T} T_c \tag{2.2}$$

$$\dot{U} = \frac{aT^*}{\left(1+\frac{I}{I_1}\right)\left(1+\frac{R}{R_1}\right)} - \frac{\lambda U}{1+\frac{U}{M_H}} - \delta_U U \tag{2.3}$$

$$\dot{D} = \frac{\lambda U}{1+\frac{U}{M_H}} - \delta_D D \tag{2.4}$$

$$\dot{A}_E = \frac{\alpha_1 M_E}{1+k_4\frac{M}{D}} - \delta_A A_E - \frac{\ln\left(\frac{1}{1-f_E}\right)}{\tau_E} A_E \tag{2.5}$$

$$\dot{E} = \frac{\alpha_2 A_E C}{\left(1+\frac{S}{S_2}\right)(C_1+C)} - \delta_E E - \frac{\ln\left(\frac{1}{1-f_E}\right)}{\tau_E} E \tag{2.6}$$

$$\dot{A}_H = \frac{\alpha_3 M_H}{1+k_4\frac{M}{(U+D)}} - \delta_A A_H - \frac{\ln\left(\frac{1}{1-f_H}\right)}{\tau_H} A_H \tag{2.7}$$

Table 1
Model variables.

Variable	Description
T_g	Tumor cells that are not killed by chemotherapy
T_c	Tumor cells killed by chemotherapy
U	Unlicensed dendritic cells
D	Licensed dendritic cells
A_E	Activating effector T cells
E	Mature effector T cells
A_H	Activating helper T cells
H	Mature helper T cells
A_R	Activating Tregs
R	Mature Tregs
C	Concentration of IL-2 in mM
S	Concentration of TGF-β in mM
I	Concentration of IL-10 in mM

$$\dot{H} = \frac{\alpha_4 A_H C}{\left(1+\frac{S}{S_2}\right)(C_1+C)} - \frac{\alpha_7 HS}{S_3+S} - \delta_H H - \frac{\ln\left(\frac{1}{1-f_H}\right)}{\tau_H} H \tag{2.8}$$

$$\dot{A}_R = \frac{\alpha_5 M_R}{1+k_4\frac{M}{D}} - \delta_A A_R - \frac{\ln\left(\frac{1}{1-f_R}\right)}{\tau_R} A_R \tag{2.9}$$

$$\dot{R} = \frac{\alpha_6 A_R C}{(C_1+C)} + \frac{\alpha_7 HS}{S_3+S} - \delta_R R - \frac{\ln\left(\frac{1}{1-f_R}\right)}{\tau_R} R \tag{2.10}$$

$$\dot{C} = \frac{p_C A_H}{\left(1+\frac{S}{S_4}\right)\left(1+\frac{I}{I_2}\right)} - \frac{C}{\tau_C} \tag{2.11}$$

$$\dot{S} = p_1 R + p_2 T - \frac{S}{\tau_S} \tag{2.12}$$

$$\dot{I} = p_3 R + p_4 T - \frac{I}{\tau_I}, \tag{2.13}$$

where

$$\gamma_1 = \gamma T_1^{m-1}, \tag{2.14}$$

and

$$T^* = \frac{T}{\left(1+\left(\frac{T^{1-n}}{k_1}\right)^p\right)^{1/p}}. \tag{2.15}$$

In order to properly incorporate the separate effects of chemotherapy killing and the cytostatic effect, the total population of tumor cells (T) from the original model has been split into two sub populations: T_g (Eq. (2.1)) is the number of cells that undergo cytostasis, survive cycles of treatment, and continue to grow; and T_c (Eq. (2.2)) is the number of cells which are killed by chemotherapy. At the start of each round of therapy, $f_T T_c$ cells are instantaneously removed from the variable T_g and added to the variable T_c, where f_T is the fraction of tumor cells killed in that particular round of chemotherapy. This split is necessary to model the short-term dynamics of the system during chemotherapy. The dying cells continue to contribute to the molecular concentrations and the effective tumor size until they perish and are removed from the system.

Since chemotherapy is usually administered in a series of pulsed cycles, it is described in the model by several parameters. The number of cycles (N_d) and the interval between the start of each cycle (P_d) determine the periodic regimen. At the start of each cycle, the cells affected by chemotherapy are reduced by a kill fraction (f_X), which depends on the cell type (X=T, E, H or R). This reduction in cell number takes place over a specified duration (τ_x), which also may differ for the various cell types. The therapy is initiated in the model when the tumor reaches a detection size, chosen here to be $T_{ch} = 10^9$ cells. This corresponds to a round mass about 1 cm in diameter, a reasonable detection size for many solid tumors (Bouchard et al., 2002; Sahani and Kalva, 2004).

The parameter r in the immune kill term of Eq. (2.1) represents an enhanced kill ability that has been observed during chemotherapy. Experiments have shown that effector T-cell killing rates can be two to four times as effective during treatment with chemotherapy (Bergmann-Leitner and Abrams, 2001). This is modeled by setting the value of r greater than 1 during the portion of the chemotherapy cycle when tumor cells are being killed by the drug. The duration is equal to the parameter τ_T. Before and after therapy cycles, the value is set to 1. The modifier $(1-f_T)$ in Eq. (2.1) accounts for the fact that the

effector T-cell kill rate in this equation only acts on the fraction of the tumor cells that escapes the chemotherapy cytotoxicity. This avoids double-counting the death rate for cells that would be killed by either the immune system alone or chemotherapy alone. During intervals of the simulation when the chemotherapy is not active, f_T is set to zero. During the period when the drug has a cytostatic effect (duration of τ_C), Eq. (2.1) is modified by setting the first term representing tumor growth to zero, for the duration of this effect. The tumor cells are still subject to being killed by the effector T cells during this period, but their growth is paused.

The tumor cells destined to be removed by chemotherapy, T_c, follow Eq. (2.2), where $T_{c,0}$ is the number of cells set to be killed in a given cycle. This equation describes exponential decay, with parameters chosen so that the population of cells destined to die goes below one cell after the duration τ_T from the start of administration of that dose. Once the population goes below one cell, T_c is set to zero, until the next dose of chemotherapy is applied, at which point the value is reset to the new population of tumor cells that will die in that cycle. This equation is an approximation of probabilistic individual cell death within a window of time, with a specific cutoff at $t = \tau_T$.

The effect of chemotherapy on the immune T cells differs from that of tumor cells, as no cytostatic effect is applied to these cells. The equation for effector T cells (E) during treatment includes the final term to account for chemotherapy. This term reduces the population of T cells by a fraction f_E over the duration τ_E, and is only active during each pulse window of length τ_E. The term is set to zero during the times when the cytoreduction is not in effect. Analogous terms are added to Eqs. (2.5) and (2.7)–(2.10) to reflect the same type of cell kill for the other T-cell populations. The five remaining equations for dendritic cells and molecules remain unchanged from our previous model.

The model assumes that the tumor recedes symmetrically as it is killed by the chemotherapy, becoming accordingly more accessible to the immune system. In actuality, there may be a delay before dead cellular material is removed and the tumor shrinks. However, the kinetics of this process are not well-understood, so the first order assumption used in this model is that the size of the tumor scales directly and instantaneously with the number of living tumor cells.

The various effects from chemotherapy do not all end simultaneously. Tumor cell death, cell death for each of the immune populations, and tumor cell cytostasis each have their own duration time. While initially, fixed values are assumed for the fraction of tumor cells killed by chemotherapy and for the duration of cytostasis, the effects of varying them are also explored later.

As in our previous work, we use two key parameters as control parameters, the antigenicity (a) and tumor growth rate (γ). Depending on the choice of these parameters, the tumor may follow one of three behaviors in the absence of therapy. First, it may be removed by the immune system without any therapeutic intervention. Second, it may be controlled at a small undetectable size by the immune system. Third, it may grow without bound. Here, we focus only on the third type of dynamic, where the tumor will grow to reach a clinically detectable size, and thus be subject to intervention with various therapies. This limits our choice of these control parameters to the region where unbounded growth occurs when therapy is not applied.

Numerically, the simulations are run as a sequence of initial value problems. The first simulation run allows the tumor to grow until it reaches the treatment size. The values of the variables at this time point become the initial conditions for the first treatment cycle simulation, with the terms for the chemotherapeutic effect turned on. As the effects of the pulses of therapy finish, the chemotherapy terms are turned off. This procedure is repeated until all cycles are administered. After the final dose, the chemotherapy terms are turned off for the remainder of the simulation. A summary of the interactions during a cycle of chemotherapy is represented in Fig. 1.

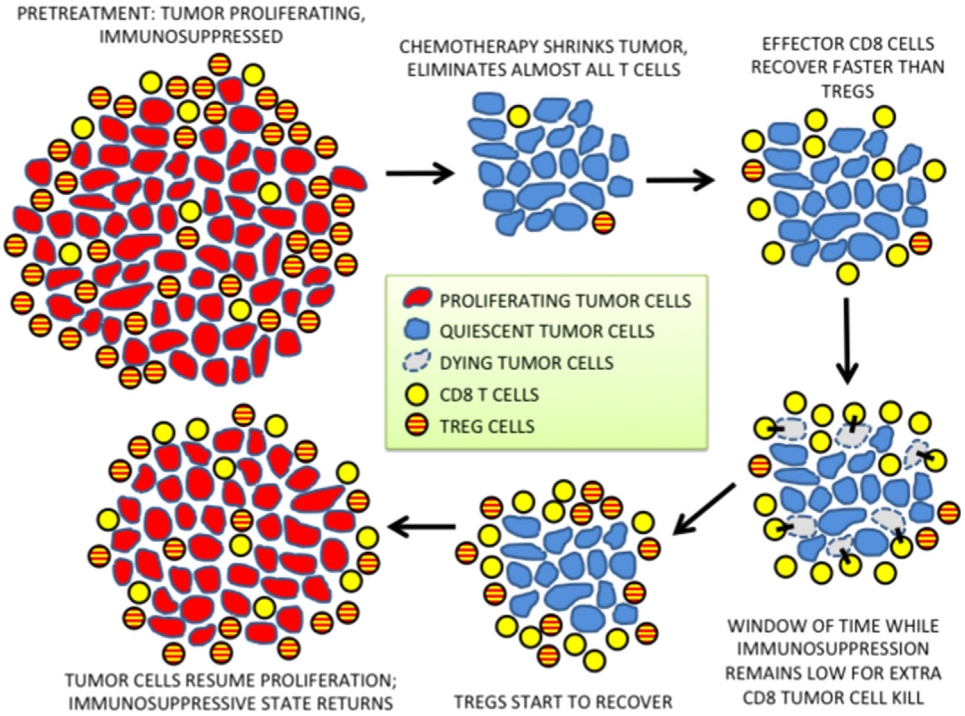

Fig. 1. A summary of the model dynamics during chemotherapy. Proliferating tumor cells (red), $CD8^+$ T cells (yellow), and Tregs (striped) are killed by chemotherapy. The tumor cells that survive are temporarily quiescent (blue). As the populations recover, T cells have the opportunity to kill susceptible tumor cells (gray). After the cytostatic period ends, the tumor regrows.

Table 2
Parameter values for chemotherapy.

Parameter	Description	Value	Units	Reference
N_d	No. of Chemo cycles	5		
P_d	Chemo cycle interval	14	days	
f_T	Kill fraction, tumor	0.70		
τ_T	Time to nadir of tumor population	5	days	Ghiringhelli et al. (2004), Ercolini et al. (2005), and Lutsiak et al. (2005)
f_E	Kill fraction, effector cells	0.70		
τ_E	Time to nadir of effector population	1.5	days	Ghiringhelli et al. (2004), Ercolini et al. (2005), and Lutsiak et al. (2005)
f_H	Kill fraction, helper cells	0.70		
τ_H	Time to nadir of helper population	1.5	days	Ghiringhelli et al. (2004), Ercolini et al. (2005), and Lutsiak et al. (2005)
f_R	Kill fraction, Tregs	0.70		
τ_R	Time to nadir of Treg population	6	days	Ghiringhelli et al. (2004), Ercolini et al. (2005), and Lutsiak et al. (2005)
τ_C	cytostatic duration	6	days	
r	Chemo-enhanced tumor kill rate	3		Bergmann-Leitner and Abrams (2001)

3. Parameter estimation

The parameters used in our previous paper (Robertson-Tessi et al., 2012) are retained for all of the simulations presented here. For convenience, tables of these parameters are reproduced in the Supplementary Material. Additional parameters pertaining to chemotherapy are given in Table 2 and used in all the simulations that follow unless otherwise noted. The parameters for kill fraction and duration were estimated from the nadir of growth curves. The cytostatic fraction was chosen to accord with the longest chemotherapeutic effect. We examine the effect of changing these estimates in the Results section.

While the goal in both this study and our previous study (Robertson-Tessi et al., 2012) was to obtain all parameter values for human breast cancer, some of the parameters had to be estimated for other cancer types, and in some cases no estimates from human studies could be located in the literature. In these latter cases, estimates were based on rodent studies. Because of significant differences in time scales between mouse and man with regard to lifespan, metabolic rate, plasma pharmacokinetics, and so forth, this raises concerns that parameters obtained from rodents may poorly reflect the clinical situation. We believe this to be less of a concern for cellular-level parameters, and primarily an issue for time-dependent parameters at the tissue or whole-body level, which in the case of the present model suggests that the main concern is the value of the parameters τ_E, τ_H, and τ_R (Table 2) giving recovery timescales for T-cell subpopulations after chemotherapy. Our estimates are based on rodent studies (Ghiringhelli et al., 2004; Lutsiak et al., 2005; Ercolini et al., 2005); however, Pircher et al. (2014) followed the time course of Treg and CD4 subpopulations in lung cancer patients after administration of cisplatin, docetaxel and cetuximab. While Pircher et al. do not explicitly give data for CD8, we note that the murine studies suggest that CD4 and CD8 populations closely track each other. Based on the data of Pircher et al., it seems that human recovery times are similar to the values we assumed for mice based on Lutsiak et al. (2005) and Ercolini et al. (2005). In particular, Pircher et al. confirm the mouse findings that effector cells recover faster than Tregs, a key aspect of the present model that leads to a window of opportunity for tumor cell kill during which immunosuppression is temporarily reduced. We have run simulations (results not shown) using values of τ_E, τ_H, and τ_R based on the data of Pircher et al. and found little difference, as the effects of varying these parameters are second-order compared to the Bergmann–Leitner effect.

In addition to chemotherapy alone, the above equations are used to simulate the following forms of chemoimmunotherapy: adoptive T-cell transfer; dendritic cell vaccination; TGF-β blockade; and Treg depletion. Adoptive T-cell immunotherapy is simulated by a single-step increase in the population of activated effector T cells (A_E) of 2×10^9 cells. This is based on the fact that typical numbers of T cells injected in the clinic range from 10^{10} to 10^{11} cells (Rosenberg et al., 1994; Dudley et al., 2002), and further that Matsui et al. (2004) found that less than 2 percent of the injected cells reach the tumor. The step increase representing the single injection is administered four days after administering one dose in the cycle of chemotherapy. The dendritic cell vaccination consists of transferring 2×10^6 dendritic cells 4 days after each cycle of chemotherapy (Brossart et al., 2000). TGF-β blockade is simulated by setting the concentration of TGF-β (S) to zero for the duration of therapy. Treg depletion in the model is simulated by reducing the Treg numbers by a predetermined fraction for each administration of the drug. This fraction can range from 40% to 90% (Barnett et al., 2005; Rasku et al., 2008); the intermediate value of 75% is chosen in our study. The reduction is accomplished by using the chemotherapy terms in the two equations for Tregs, Eqs. (2.9) and (2.10). Treg depletion therapy is usually administered in multiple doses, and the regimen used in the simulations is one cycle every two weeks, for a total of eight cycles.

4. Results of the model without chemotherapy

In our previous study, the effects of two main parameters, tumor growth rate and tumor antigenicity, were considered. Tumor antigenicity was the coefficient for the CD8-induced tumor-cell kill rate, which in actuality reflects both the effectiveness of the CD8 cell killing and the extent to which the tumor attracts these cells. The model included tumor cells and 11 types of immune cells: unlicensed and licensed dendritic cells, and 3 categories of T cells, each with memory, activated, and fully functional forms: helper (CD4+) T cells, effector (CD8+) T cells, and Tregs (regulatory T cells). Two key cytokines, the immunostimulatory IL-2 and the immunosuppressive IL-10, were included, as well as TGF-β, arguably the most important immunosuppressive factor produced by the tumor.

A system of 12 coupled ordinary differential equations with 43 parameters described the interactions between these model components. Values for most of the parameters were obtained from the literature, for the case of human breast cancer where possible, but in some cases only values from rodent experiments could be found. The model accounted for reduced access of the T cells to the tumor. The immunosuppressive factors TGF-β and IL-10 were produced by both tumor cells and Tregs. One immunosuppressive effect included in the model was the conversion of helper cells to Tregs induced by TGF-β. Also, maturation of dendritic cells was inhibited by both IL-10 and Tregs. Both TGF-β and Tregs act to reduce the tumor killing rate of the effector T cells.

The model showed that if tumor growth rate is not too high, tumor control is possible for an intermediate range of antigenicity, but

is lost if antigenicity is either too low or too high. At higher antigenicity, tumors escape because of the large increase in Treg populations and TGF-β levels. The finding of an optimum intermediate antigenicity has significance for therapies aimed at increasing tumor antigenic expression. The effects of removing several mechanisms of immunosuppression were then examined. It was found that the tumor control region would expand significantly and there would no longer be an optimal antigenicity. Eliminating just the TGF-β-induced conversion of helper T cells to Tregs also made the optimal antigenicity disappear, and increased the control region, although not as much as complete removal of all effects of TGF-β. Thus therapies targeting TGF-β stand a chance of being effective. In contrast, Il-10 was found to have far less of an immunosuppressive effect, for production rates found in the literature.

Dendritic cell therapy, where the cells are exposed to tumor antigen in vitro and then reinjected into the patient, was also modeled. It was found that multiple cycles would be needed to remove a tumor, assuming no development of resistance, and that an optimal interval of time between treatment cycles exists. Removal was only possible for lower tumor growth rates. At intermediate growth rates, it is only possible to contain the tumor at a finite size, which will grow once treatment is terminated. At higher growth rates, no control is possible. An interesting finding of the model is that a strongly immunosuppressed phase ensues after treatment is ceased, because the effector T cell population falls much faster than the Treg population. During this transient phase, tumor growth is higher than it would have been in the absence of treatment. This suggests that dendritic cell therapy, if it cannot be continued indefinitely, should perhaps be ramped down gradually. As with increasing antigenicity, a somewhat surprising finding was that increasing the number of dendritic cells injected on each cycle eventually led to tumor escape.

Overall, the main findings of the paper are that therapies targeting TGF-β and/or Tregs have potential to be effective, and that targeting IL-10 is far less promising. Increasing tumor antigen expression or the quantity of dendritic cells does not always improve response, as there are optimal levels. These findings are important as they suggest that the appropriate form of immunotherapy may depend strongly on where in the antigenicity-growth rate plane the tumor initially lies. The fact that the outcome of therapy depends on the individual characteristics of a patient's tumor, that is, on where a patient initially lies in the parameter space, suggests that immunotherapy has the potential to be improved with individualized approaches.

5. Chemotherapy

5.1. Effect of chemotherapy on immunosuppression

Fig. 2 shows the progression of a representative tumor that has undergone chemotherapeutic treatment. The treatment intervals are shown by the gray rectangular bars, with each bar indicating one of the five doses of chemotherapy. The plots begin shortly before the tumor reaches the treatment size T_{ch}. In this particular case, the tumor continues to grow without bound, since it is not cured by the therapy.

Chemotherapy changes the quantity of cells in the system on the order of days. At the start of the first chemotherapy dose, the tumor is at the treatment size (10^9 cells), and the immune system is highly suppressed by the presence of Tregs and TGF-β. Access to the interior of the tumor is limited at these sizes due to the lack of full perfusion. Upon the application of therapy, the tumor cells and T cells are reduced in number, as seen in Fig. 2a. The TGF-β levels are rapidly reduced (not shown), since there are fewer tumor cells and Tregs present to produce this molecule. The half-life of TGF-β is shorter than a day; consequently, the TGF-β levels decrease in tandem with cellular killing during treatment.

The effector T cell-to-Treg ratio can vary on short timescales, due to the difference in killing rates of these cells by the chemotherapy. Effector cells reach their nadir sooner than Tregs (Lutsiak et al., 2005), so the ratio initially decreases, as shown in Fig. 2b. When the Treg nadir is reached, the ratio is maximal and therefore the immune system will have the most effect on the tumor.

Fig. 2c shows that the fraction of Tregs which originate from helper T cells becomes smaller. This is due to the fact that TGF-β levels are reduced, and therefore the converted cells are not rapidly replenished following treatment.

Fig. 2d shows the suppression due to Tregs, TGF-β, and access limitation. The suppression at the treatment size is high, with Tregs and access limitation providing significant barriers to any significant immune response. After the first cycle, Treg suppression is reduced rapidly, and then begins to rebound (dashed line in Fig. 2d). This pattern repeats during the next few cycles. Even though the suppression due to Tregs is reduced by the therapy compared to the pre-treatment levels, the Tregs remain a significant source of suppression throughout the treatment. This is expected, since the Tregs and T cells are reduced by the same fractions; the variations in Treg suppression are due to the different timescales with which the Tregs and the other T cells are killed by the chemotherapy, as well as their different expansion rates. The nadir of Treg suppression occurs over 20 days after the final dose is administered. Typically, the transients of the model last for a few weeks, and then the model reverts to pretreatment behavior, assuming that a cure has not been attained.

Unlike Treg suppression, TGF-β-induced suppression and access limitation are steadily reduced with each chemotherapy dose (dashed and dash-dotted lines in Fig. 2d). After the third dose, both of these effects have been reduced to insignificant levels for the remainder of the treatment and for some weeks beyond. Therefore, the overall suppression after the third cycle of treatment is almost entirely due to Tregs. This suggests that if Treg suppression could be lessened further during the later cycles of chemotherapy by a concurrent immunotherapy, the effects of the immune system would be further enhanced.

5.2. Long-term tumor outcome with chemotherapy

Chemotherapy is simulated with short-term changes to the model equations and parameters; these changes are in effect only within the treatment time windows. Once chemotherapy-induced cell kill is complete, the governing equations revert to the pre-treatment state and the phase plane analysis presented in our previous work (Robertson-Tessi et al., 2012) remains valid post-treatment. However, chemotherapy causes a change of initial conditions, and therefore the behavior of the tumor can change after therapy. It is widely believed that there is a finite cure volume for tumors, based on the fact that not all tumor cells are clonogenic (Geara et al., 1991; Zeman, 2000). Chemotherapy may result in a tumor cell nadir that goes below this cure volume, which we choose to be $T = 1$ cell in this work. In this case, the tumor is considered to be cured.

The direct cytotoxic effect of chemotherapy causes a delay in tumor growth which could correspond to increased survival time. This effect is shown in Fig. 3 in the dashed plot. The figure also shows the additional delay time of approximately 6 months caused by the effect of chemotherapy on transient tumor–immune interactions (solid line). This result suggests that the immune system plays a significant role in tumor response that cannot be attributed to the direct cytotoxicity of chemotherapy alone.

Clinical tumors show a range of antigenicities and growth rates; therefore it is of interest to investigate how these parameters affect the efficacy of chemotherapy. Fig. 4 shows the results of chemotherapy

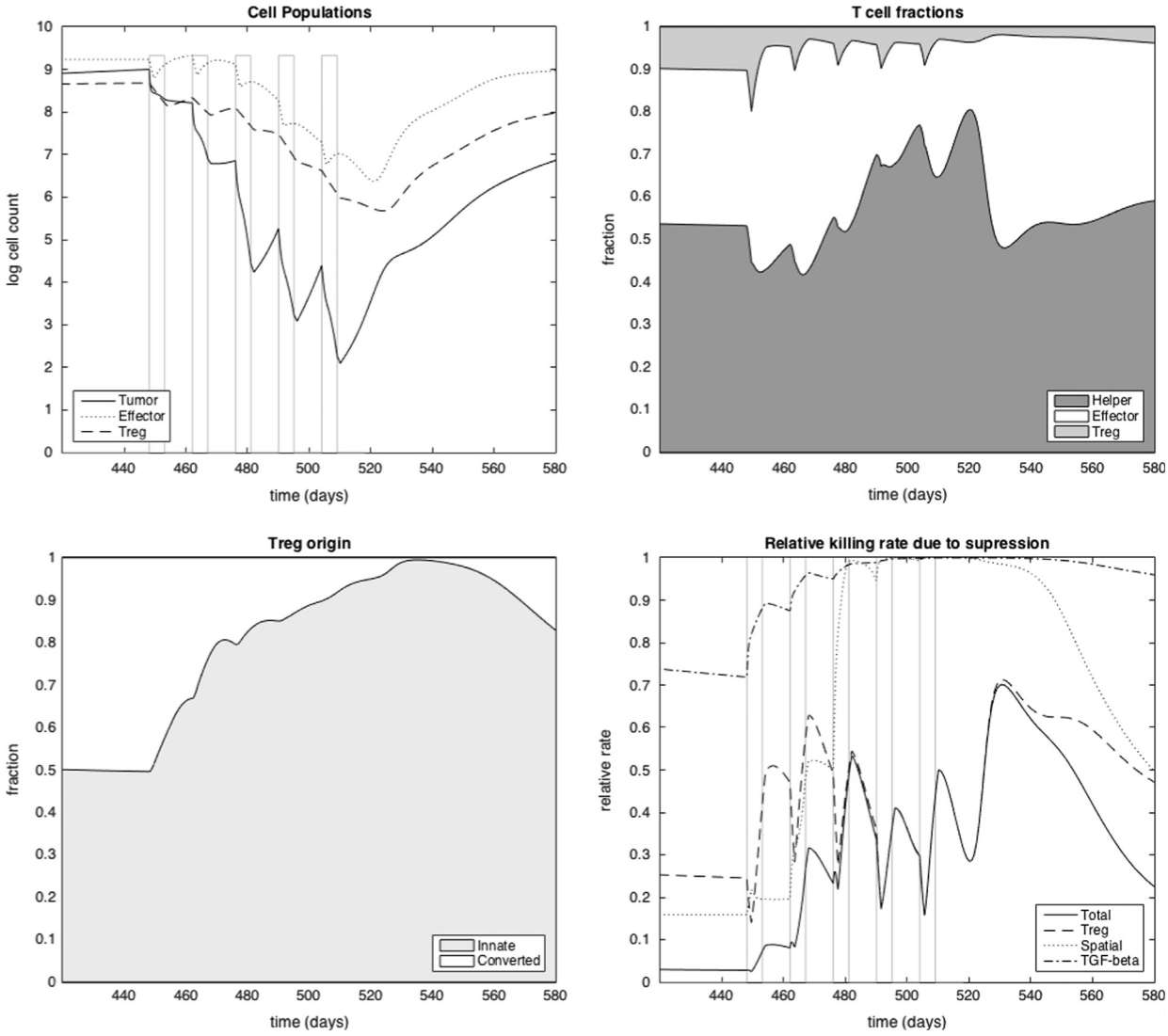

Fig. 2. The effects of chemotherapy on a tumor and immune cells are shown. The tumor has an antigenicity $a=1$/day and a growth rate of $\gamma=700/\text{cell}^{0.5}$/day. The chemotherapy regimen chosen here is 5 cycles, 14 days apart. Seventy percent of tumor and T cells are killed on each of the 5 cycles. The gray rectangular bars indicate the individual administrations of chemotherapy doses. (a) Cell populations over time, (b) T cell fractions, (c) Treg origination, and (d) suppression of tumor cell killing rate.

applied to a range of tumor types with varying antigenicities (horizontal axis) and growth rates (vertical axis). Tumors that reach a typical clinical detection size of 10^9 cells are treated with the chemotherapy regimen as given in Table 2. There is one area where the tumors have been fully removed after chemotherapy, marked *Removal by Treatment*. It is worth noting again that these tumors cannot be removed by direct cytotoxicity of chemotherapy alone; if the immune system were not active, the chemotherapy would leave behind several million viable tumor cells after the last cycle. The immune system is necessary for the complete removal of the tumor.

The dashed lines in Fig. 4 are contours of equal increase in survival time due to therapy. The increase in survival time is calculated as the difference in time it takes the tumor to reach an endpoint size of 10^{11} cells with and without chemotherapy. The left axis shows the increase in survival time that would be gained by chemotherapy alone for the chosen parameters, in the absence of the immune system. This distribution of times depends only on the tumor growth law. For low values of antigenicity, the survival contours approach these axis values, since the effect of the immune system is minimal. At a fixed tumor growth rate, it is clear that for tumors of moderate antigenicity or higher, survival times can be extended threefold or more by the combined action of the chemotherapy and the immune system as compared to direct cytotoxicity due to chemotherapy alone.

The contours also show that there is an optimal antigenicity for maximizing the survival time resulting from treatment. This optimal antigenicity lies within the range of 10^{-2} to 10^{-1}/day. However, in contrast to the case where there is no chemotherapy, there is a range of antigenicities where both increasing and decreasing the antigenicity would lead to improved outcomes. For example, if a tumor has a growth rate of $\gamma=600/\text{cell}^{0.5}$/day, the best outcome (removal) would be attained by increasing the antigenicity to very high levels. However, if that is not possible, the second choice (palliative treatment) would be to approach the optimal antigenicity and maximize the survival time. While the model is not intended to make predictions for specific tumor types, this example illustrates that the interactions between a tumor, the immune system, and treatment are non-linear, and often not intuitively obvious. Simulations also showed the counterintuitive result that minimizing the tumor nadir is not synonymous with maximizing survival time, except when the tumor nadir is below the cure volume. This result is consistent with clinical findings that extent of tumor regression does not always predict increased survival time.

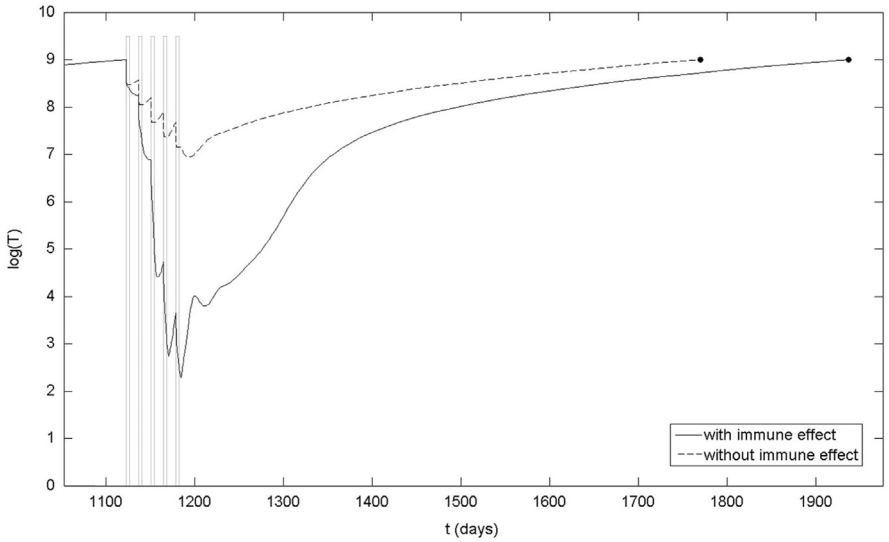

Fig. 3. Two representative simulations showing the effect of the immune system during chemotherapy. The chemotherapy regimen is parameterized in Table 2. The tumor has an antigenicity of $a=10$/day, and the tumor growth rate is $\gamma=500/\text{cell}^{0.5}$/day. Both simulations are equivalent until the treatment is administered when $T=10^9$ cells. The solid line shows the tumor progression when the chemotherapy regimen is administered with the immune system functioning normally. The dashed line shows the progression when the same regimen is administered, but the parameter r_0 is set to 0 for the duration of the treatment, which turns off the killing of tumor cells by T cells. The parameter is reset to its normal value at the end of the chemotherapy regimen. The action of the immune system during chemotherapy is responsible for almost 6 extra months of regrowth time, as shown by the endpoints when the tumor regains the treatment size.

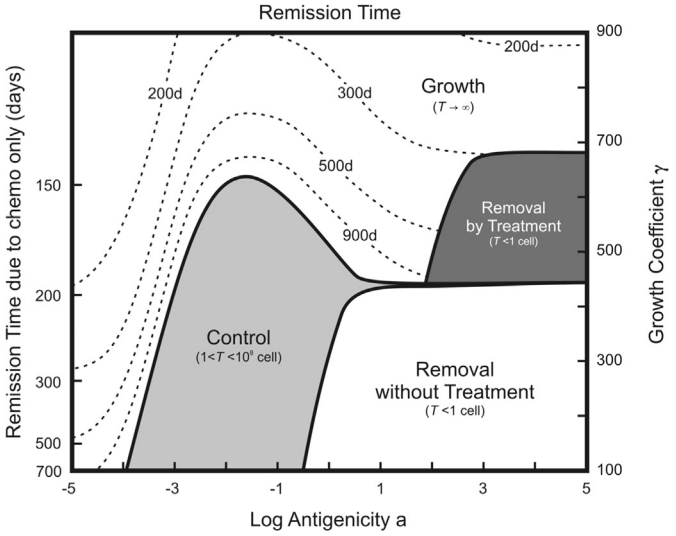

Fig. 4. Tumor responses to the immune system, with chemotherapy. *Growth* denotes tumor growth which is unbounded, *Removal without Treatment* denotes complete cure of the tumor by the immune system before the treatment size is reached, *Control* denotes maintenance of the tumor at a small but steady size, and *Removal by Treatment* denotes tumors which escaped the immune system prior to treatment, but were removed by the immune system following chemotherapy. The dashed contours show the increase in survival time for those tumors that regrew. Increase in survival time is calculated as the difference between the time needed to reach an endpoint size of $T=10^{11}$ cells, with and without chemotherapy.

5.3. The effect of varying chemotherapy parameters

The model incorporates several consequences of chemotherapy which have been seen in experimental studies. The enhanced killing of tumor cells by effector T cells during the delivery of the chemotherapy is one beneficial "side effect" that has been observed (Bergmann-Leitner and Abrams, 2001), represented by the parameter r in Eq. (2.1). Dependence on the parameter r is shown in Fig. 5a. This enhancement of killing rate has a large effect on the outcome of highly antigenic tumors, but does not change the curability of tumors with moderate antigenicity. Changing this parameter alone does not have a great effect on survival times. The survival times are increased somewhat with increases in the parameter r, but the increases are marginal (not shown). This is due to the fact that the nadir reached after treatment is almost always less than 10^5 cells. The regrowth times of a tumor at these small volumes are relatively quick, due to the quasi-exponential nature of its growth; therefore, the difference between reaching a nadir of 10^2 versus 10^4 cells at the end of treatment does not significantly extend the regrowth time. In contrast, Fig. 3 showed a difference in nadir between 10^2 and 10^7 cells, which results in over 5 months of extra regrowth time.

While cytostatic drugs on their own only postpone tumor cell growth by a short time period, when coupled with immune effects they can provide a large benefit in terms of tumor reduction. During the period of cytostatic effect, the tumor size can only decrease due to killing by immune system cells. Fig. 5b shows the effect of varying the cytostatic duration. As with the enhanced killing rate, the primary change is that increased cytostatic duration results in better curability for highly antigenic tumors. Survival times are marginally affected, for the same reasons outlined above.

The assumed fractional kill from direct effects of chemotherapy could of course be increased by increasing the drug dose on each cycle. However, the fraction cannot be raised arbitrarily high *in vivo*; toxicity limits the dosing of these drugs, and nearly all drugs show diminishing returns with increasing dose. The effect of changing the fractional kill parameters f_X, for the same chemotherapy regimen, is shown in Fig. 5c. The results show that changes in kill fraction can have a significant effect on the outcome of chemotherapy, extending the therapeutic effect. It is important to note that the changes in kill fraction apply to tumors cells and T cells equally, meaning that all these populations are reduced proportionally. The primary advantage to increased fractional kill is that a rapid reduction of the tumor burden diminishes the TGF-β suppression and removes the access limitation restriction more quickly. The system enters a state of reduced immunosuppression faster when the fractional kill is higher. Host toxicity constrains the maximum kill fraction, so in practice fractional kill may not always be an adjustable therapeutic variable.

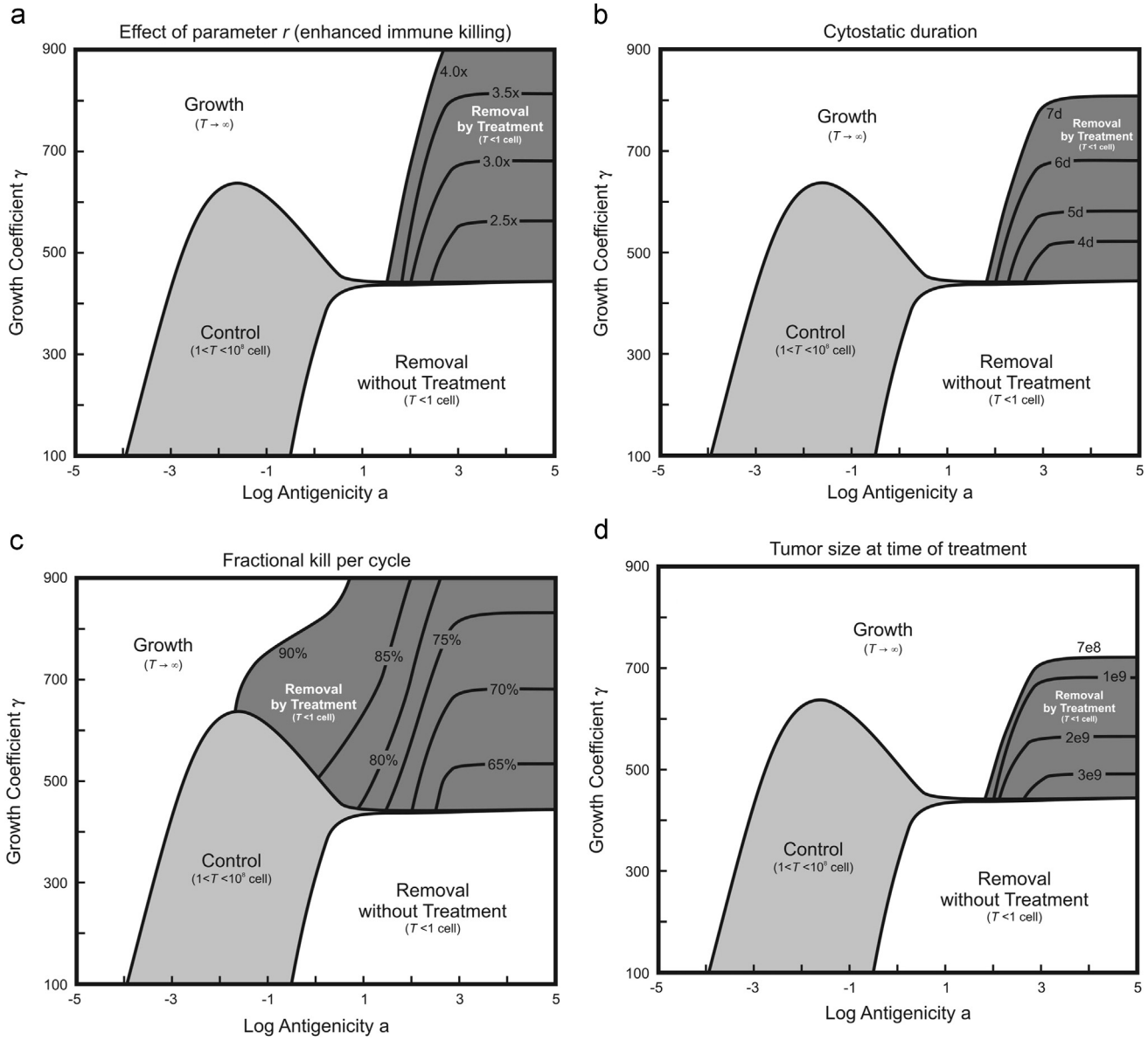

Fig. 5. (a) The results of varying the parameter r in the simulations are shown. The solid contours show the boundary of the cure zone for a given value of r. As the parameter r is increased, faster-growing tumors can be cured by the chemotherapy. However, the effect on tumors with lower antigenicity is minimal. (b) The effect of varying the cytostatic duration is shown. The solid contours show the boundary of the cure zone for a given cytostatic duration, in days. As with the enhanced killing parameter, changes in the cytostatic duration primarily allow the chemotherapy to cure more aggressive tumors of high antigenicity. (c) The effects of cellular kill fraction by chemotherapy are shown. The solid contours show the boundary of the cure zone for a given kill fraction. Changing the fraction of cells killed per cycle of chemotherapy has a significant effect on the curability region, extending the cure region to moderately antigenic tumors with fast growth rates. (d) Application of the same chemotherapy regimen at different tumor sizes is shown. The solid contours show the boundary of the cure zone when the same treatment is applied at the indicated tumor size. The notation 7e8 represents 7×10^8 cells. Although detection at smaller sizes improves the chances of removing the tumor, the effect is restricted to highly antigenic tumors.

Early detection is often cited as a major advantage when treating tumors (Smith et al., 2002), and it has been argued that because of drug delivery issues, chemotherapy would have a greater effect on a smaller tumor (Abe et al., 1985). Results from changing the detection size (Fig. 5d) suggest that there is a limited benefit to early detection in the context of immune system. The effect on moderate- to low-antigenic tumors is minimal with respect to remission time (not shown).

5.4. *Optimization of chemotherapy based on immune system response*

Chemotherapy is almost always administered in multiple fractionated cycles. The effect of varying the interval and number of cycles under the constraint of constant total dose is explored with the model. Although the individual cycles need not be of the same dose, it is assumed here that they are, so that the total dose is divided equally among them. Since kill fraction varies with dose, regimens with more cycles will kill fewer cells per cycle. Table 3 shows the fractional cell kill per delivery of the given division of the total dose, estimated from cell survival curves (Levasseur et al., 1998). The values were derived for doxorubicin with a total dose of 1 μM at 6 h of exposure.

Table 3 shows the fraction of cells killed as a function of fractional chemotherapy dose, estimated from experimental data (Levasseur et al., 1998).

Fig. 6 shows the results of varying the schedule and dosing. The number of cycles is given on the horizontal axis. These numbers also correspond to the reciprocal of the fraction of the total dose administered. The vertical axis is a measure of the relative

Table 3
The fraction of cells killed as a function of fractional chemotherapy dose (Levasseur et al., 1998).

Fraction of total dose	1	1/2	1/3	1/4	1/5	1/6
Fraction of cells killed	0.98	0.93	0.86	0.78	0.70	0.62
Fraction of total dose	1/7	1/8	1/9	1/10	1/12	1/14
Fraction of cells killed	0.55	0.49	0.43	0.38	0.30	0.24

curability, on an arbitrary scale. For a given chemotherapy regimen, this value is determined by measuring the area of the *Removal by Treatment* zone relative to the total area of the rectangular region of parameter space considered here. Each trace on the plot corresponds to a different treatment interval between doses, varying from 12 to 18 days, corresponding to typical cycle intervals used in the clinic. Intervals longer than 18 days produced no cure regions.

Fig. 6 shows that the maximum number of tumor types that are cured by the immune system for a given schedule varies with how the total dose is split up. There is an optimal number of cycles for any given dosing interval, which exists between the extremes of a single bolus injection and very low dose metronomic delivery. When the full dose is given in too few cycles, the immune system does not have enough opportunity to kill the tumor, despite the high fractional kill of the chemotherapy. Conversely, when the dosing is split into too many small fractions, the chemotherapy does not kill enough tumor cells per treatment cycle to reduce the immunosuppression significantly.

The figure also shows that reducing the time between dose cycles is greatly beneficial. The reduction of immunosuppression during a cycle of chemotherapy leads to enhanced immune cell killing of the tumor, which in turn benefits subsequent cycles of chemotherapy, resulting in a positive feedback. Dose-dense therapy, in which the cycles are delivered closer together than the standard practice, has been found to improve survival rates (Citron et al., 2003). This has previously been explained using growth kinetics alone (Norton, 2001). The model presented here shows that the benefits of dose-dense therapy may be partially explained by immune effects.

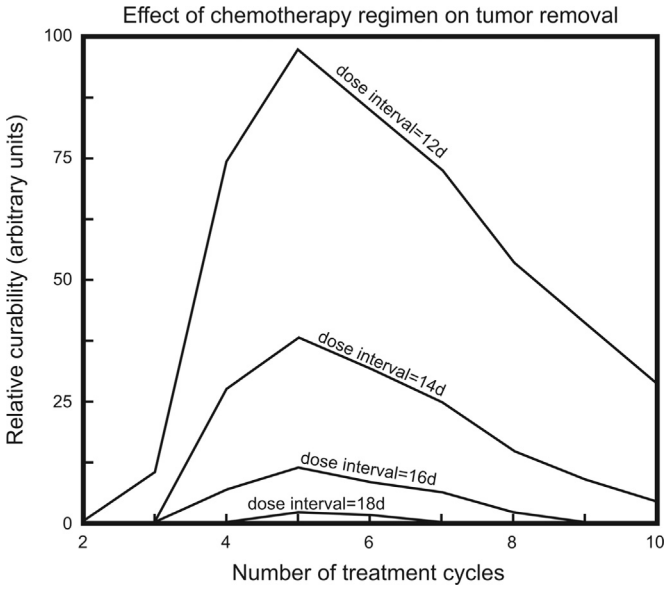

Fig. 6. For a given total dose of chemotherapy drug, the results of dosing schedule are shown. The relative curability is calculated by measuring the area of the *Removal by Treatment* zone for different regimens of therapy. The horizontal axis shows the number of treatment cycles. Since the total dose (summed over all cycles) is constant, the dose per cycle decreases as the reciprocal of the total number of cycles. The fractional kill per cycle is dependent on the dose size, and values are given in Table 3. Each trace on the plot corresponds to a different interval between doses. A chemotherapy regimen with 5 cycles appears to maximize the effect of the immune system.

6. Chemoimmunotherapy

As indicated by the above results, chemotherapy is insufficient to cure many tumors, even when immune effects are taken into account. However, the results also suggest that interventions to increase anti-tumor effects of the immune system might make a significant difference to the outcome of therapy. This motivates combining chemotherapy with immune interventions with the hope of increasing the tumor control region further.

A long-held belief is that chemotherapy and immunotherapy work at cross purposes, because the former usually induces leukopenia. This view has recently been questioned by at least some investigators (Weir et al., 2011; Gameiro et al., 2011). Most preclinical and clinical chemoimmunotherapy studies still separate chemotherapy from immunotherapy in time, or use low-dose chemotherapy with the expectation of an immunological rather than direct cytotoxic effect. Yet it is unclear whether avoidance of combining full-dose chemotherapy simultaneously with immunotherapy is indeed necessary or optimal. As noted by Emens et al. (2001), "drugs traditionally used for tumor cytoreduction can have both positive and negative effects on host immunity." On the one hand, Schlom (2012) notes that clinical response to vaccines has been more favorable in patients who have experienced fewer prior chemotherapy cycles, or who have a longer interval of time between the last cycle and the administration of vaccine. The study of Gardner et al. (1993), which showed long-lasting detrimental effects of a variety of standard chemotherapeutic drugs on stem cells' ability to produce circulating lymphocytes, likewise appeared to contraindicate the combination of chemotherapy with immune stimulation. On the other hand, Casati et al. (2005) found that doxorubicin and melphalan did not disrupt the immunogenicity of dendritic cell vaccines. McCoy et al. (2012) found that while chemotherapy depleted T cells, they recovered rapidly, and at the end of each treatment cycle the percentages of proliferating cells were higher than before the start of treatment. Such findings motivate the mathematical modeling of normal-dose chemotherapy combined with immunotherapy. Indeed, even high-dose chemotherapy has been combined with immunotherapy for hematological malignancies, as reviewed by Liseth et al. (2010).

In this section, some clinically relevant immunotherapies in combination with cytotoxic chemotherapy are investigated. These immunotherapies involve either boosting anti-tumor immune cells and cytokines in the body, or reducing the immunosuppressive ones. Two of the former type, namely dendritic cell injection and adoptive T-cell transfer therapy, will be modeled here, as well as two of the latter type, namely TGF-β blocking and Treg depletion.

6.1. Treg depletion

Tregs have been implicated in many studies as a major source of tumor-induced immunosuppression (Curiel, 2007). Treg depletion has been proposed as a novel therapy to enhance immune system effects. For example, one drug used to deplete Tregs is denileukin diftitox, which is a synthesis of diphtheria toxin with IL-2 (Foss, 2006). With the present model, simulations of Treg depletion administered alone showed a reduction in tumor size of less than 70% (results not shown), comparable with the 50% reductions seen in the best clinical results (Barnett et al., 2005; Rasku et al., 2008).

Fig. 7 shows the outcome of combining the chemotherapy regimen and Treg depletion simultaneously. The percentages shown in the solid contours indicate the percentage of Tregs that are depleted on each cycle; cell kill by the Treg depletion therapy and by chemotherapy are assumed independent of each other. The cure region is significantly expanded with the addition of Treg depletion therapy. The zone marked 0% represents the cure zone with the chemotherapy alone. Treg depletion administered alone was unable to fully cure any tumor (results not shown), but in combination with chemotherapy the treatment contributes to significant gains in curability. In addition to direct cytotoxicity, chemotherapy contributes to tumor control by reducing the Treg population, and the addition of a targeted Treg depletion drug reduces this population further, increasing the positive feedback between chemotherapy and immune effects.

6.2. TGF-β blockade

Another avenue for reducing tumor-induced immunosuppression is the blockade of TGF-β. Here we model the best-case scenario of an agent such as a TGF-β receptor kinase inhibitor (Suzuki et al., 2004; Uhl et al., 2004), where the effect of TGF-β is completely abrogated by the therapy both in the plasma and in the tumor.

Blocking TGF-β in the model showed very little effect (results not shown). A slight increase of effector cell numbers was apparent, but it had no significant effect on tumor progression. Because Tregs are the primary factor dampening the immune anti-tumor effects, the loss of TGF-β does not cause a significant change to the overall immunosuppression. Even though some of the Tregs arise from TGF-β-induced conversion from helper cells, this does not have a significant effect on Treg cell counts over the short timescale of the treatment. In general, the T-cell numbers are well-established at the time of treatment, and removal of only one immunosuppressive element has little effect. Combination of TGF-β blockade with chemotherapy showed a modest increase in the cure region compared to chemotherapy alone (results not shown). This increase was seen only for highly antigenic tumors. This is partially explained in Fig. 2, which shows that TGF-β suppression is insignificant after the third cycle of chemotherapy. Therefore, the immunotherapy only has an effect on the early stages of treatment.

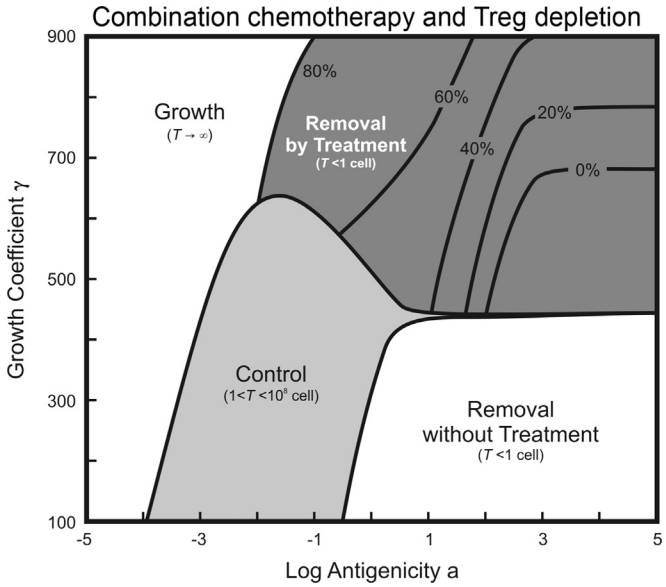

Fig. 7. Chemotherapy and Treg depletion administered concurrently. The chemotherapy regimen is the same as described for Fig. 4. Treg depletion therapy depletes a percentage of the Treg cells, as shown indicated on the contours. The combination therapy shows much greater effect on tumor outcome than either therapy alone.

Benefits from combining TGF-β inhibition with chemotherapy have been noted in pre-clinical rodent model studies. Bandyopadhyay et al. found that combining the TGF-β type I receptor kinase inhibitor TbRI-KI with doxorubicin in a mouse model was more effective at reducing tumor growth than doxorubicin monotherapy (Bandyopadhyay et al., 2010). While they attributed this benefit to inhibition of doxorubicin-induced epithelial-mesenchymal transition, it is possible that the mechanisms suggested by the present model also contributed. Similarly, Bhola et al. (2013) found significant increased growth inhibition of mouse xenograft tumors when the TGF-β type I receptor kinase inhibitor LY2157299 was used in combination with paclitaxel. The effect was conjectured to be due to TGF-β increasing stem-like properties of tumor cells and thus making them more resistant to chemotherapy. Yet another xenograft study (Liu et al., 2010) found that TGF-β significantly enhances the anti-tumor effects of doxorubicin liposome treatment; in this case, it was attributed to improved drug delivery following on blocking TGF-β-induced production of collagen by stromal cells. The results of these studies are consistent with the increased region of tumor control seen in the present simulations.

6.3. Dendritic cell therapy

Another immunotherapeutic intervention that has been used in clinical trials is dendritic cell vaccination (Chu et al., 2012; Akiyama et al., 2012). In our previous work (Robertson-Tessi et al., 2012), dendritic cell vaccination monotherapy was found to have some anti-tumor effect, but, counterintuitively, increasing the number of dendritic cells beyond a certain point was counterproductive. Here, we simulate dendritic cell vaccination administered concomitantly with chemotherapy.

Fig. 8 shows that the addition of dendritic cell therapy greatly expands the cure region compared to chemotherapy alone, although the effect decreases as antigenicity becomes large. When antigenicity is low, the immune system is unable to take advantage of the benefits of chemotherapy alone; therefore dendritic cell therapy provides a complementary boost to the immune cell populations. However, when antigenicity is high, immunosuppression is the limiting factor, and adding more dendritic cells has a minimal effect under such conditions. Thus, it is not clear that more intrinsically immunogenic tumors will always have a better response to this type of therapy. The expansion of the cure zone is consistent with clinical findings of Castillo et al. (2012) who reported a significant increase in the percent of pathological complete responses for HER2neu-negative breast cancer patients. Castillo did not report the exact schedule of the treatment, thus, it is unclear how comparable it was to the regimen assumed in the present simulations. Encouragingly, Castillo et al. reported no additional toxicity from the dendritic cell vaccine, confirming the feasibility of adding such vaccines to normal-dose chemotherapy.

Note that even in some regions of Fig. 8 where the tumor is not completely controlled, the regrowth time of the tumor is extended. This may explain the findings of Wheeler et al. (2004) who studied the effect of giving chemotherapy after vaccination for glioblastoma, and found that chemotherapeutic responses had significantly longer duration for vaccinated patients.

6.4. Adoptive T-cell transfer

Adoptive T-cell transfer therapy involves removing T cells from the cancer patient, selecting those which are tumor specific, expanding the population in vitro, and then reintroducing them into the patient (Rosenberg et al., 1994; June, 2007). This therapy

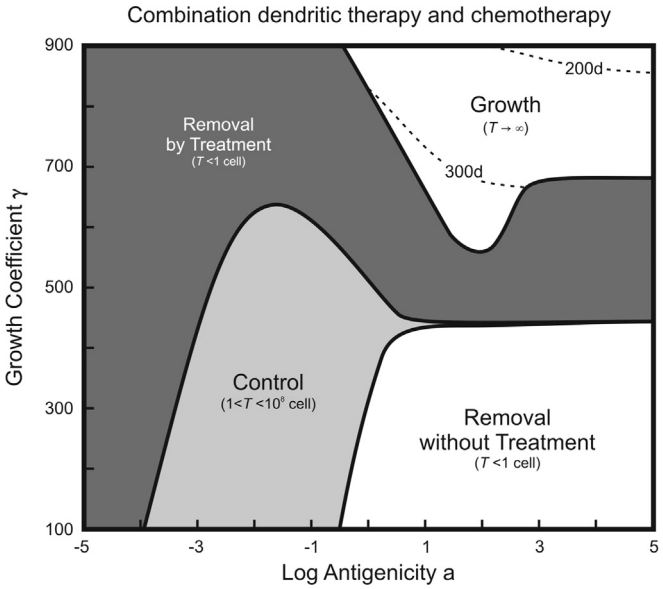

Fig. 8. Dendritic cell therapy is administered concurrently with chemotherapy. A large range of tumors is cured with the combination of both therapies.

seeks to bypass the suppression of T-cell proliferation, but in contrast to IL-2 therapy, the effector cell population is expanded without concomitantly expanding the Tregs. The maximum number of T cells may be limited by patient toxicity combined with the fact that, at least according to murine studies, less than 2 percent of the T cells reach the tumor (Matsui et al., 2004). In simulations of adoptive transfer therapy in the absence of chemotherapy (results not shown), the transferred T cells are found to persist anywhere from 2 to 8 weeks, depending on their initial level at the time of treatment. This is in agreement with the T-cell counts measured in Dudley et al. (2002). In two patients from that study, the transferred cells persisted from 3 to 4 weeks. However, no tumors of any type are cured in our simulations which is consistent with the clinical study of Dudley et al. (2002)

Fig. 9 shows the results of administering adoptive T-cell therapy during a course of chemotherapy. Panel (a) shows tumor outcome, with the cure region in medium gray and uncured region in light gray. The black region is where tumors do not reach detectable size. Panel (b) shows the area of the cure zone in the (antigenicity, growth rate) parameter space divided by the total possible cure area, for varying total number of chemotherapy cycles and for varying time between cycles. It is assumed that clinical feasibility limits adoptive T-cell therapy to a single treatment; the rows of panel (a) and horizontal axis of panel (b) show how the outcome changes depending on which cycle of the chemotherapy the T-cell therapy is administered in, varied from cycle 1 to cycle 5. For all chosen values for the length of the time interval between chemotherapy cycles, the maximum removal region is achieved when T cells are given at cycle 4, as shown by the peak of maximal cure zone area in Fig. 9b. When the T cells are given too early, their benefit is limited by the high degree of immunosuppression as well as the access problems associated with a larger tumor. However, if the T cells are injected too late (at the last cycle), the cells have only one cycle to benefit from the various immunogenic benefits of chemotherapy, namely the enhanced tumor lytic power of the T cells that is seen post-chemotherapy (Bergmann–Leitner effect), the cytostatic effect, and the altered immunosuppression.

Proceeding up the columns of Fig. 9a shows the effect of "dose-dense" chemotherapy, that is, reducing the interval of time between chemotherapy cycles. While clinical results showing a benefit from dose-dense therapy (Citron et al., 2003) have purportedly been explained solely in terms of Gompertzian growth kinetics (Larry and Simon, 1986), in fact growth kinetics alone cannot mathematically explain this phenomenon under the Norton–Simon assumption that chemotherapy kill fraction is proportional to the fraction of growing cells in a tumor; this holds true for both exponential and Gompertzian growth law models, and indeed any growth law model where the rate of growth depends only on the current tumor volume and not on any other function of time. The inclusion of immune effects gives a mechanism for fractional kill to increase as tumor size becomes smaller, and this may be the main factor explaining improved outcomes with a shorter inter-cycle time.

While the above lines of reasoning can be used to understand the changes in Fig. 9a as one proceeds either across a row or up a column, when the figure is viewed as a whole, it is clear that it reflects very complex interactions between a number of different factors. As with the earlier figures, Fig. 9 shows the net result from: the cytotoxic effect of chemotherapy; the cytostatic effect of chemotherapy; the Bergmann–Leitner effect; reduction of immunosuppression by chemotherapy; increased tumor cell kill as the tumor gets smaller because of improved access; increased tumor cell kill as immunosuppression decreases; the different time scales for recovery of the CD8 effector and Treg cell populations, and so forth. If one views each point in the growth factor-antigenicity plane as characterizing an individual tumor, then each point can also be thought of as an individual patient (note that these two parameters are assumed constant over the lifetime of the tumor). Fig. 9 shows that while the largest zone of tumor removals (that is, the largest shaded area) is achieved with the shortest inter-cycle time, and with the adoptive T cells added at cycle 4, this would only be the optimal therapy for a patient population that was uniformly distributed over the growth rate-antigenicity plane. There is no a priori reason to assume such a distribution. Moreover, for an individual patient, the optimal therapy is often not the one that coincides with that giving the largest tumor removal area. This suggests opportunities for significantly improving outcome with patient-specific treatment. Finally, Fig. 9a shows that nearly every point in the plane (that is, nearly every tumor type) can be removed by one of the 20 possible regimens explored. This suggests that if a patient has failed chemoimmunotherapy, it may not be appropriate to assume that their tumor is too poorly antigenic and that immunotherapy should not be tried further. Rather, it may simply be a matter of changing the regimen to achieve a successful outcome.

Fig. 9 was produced without adding any therapeutic IL-2. It is common clinical practice to administer high-dose IL-2 to patients receiving adoptive T-cell transfer. The same set of simulations from Fig. 9 was also performed using concurrent administration of various levels of IL-2, but we found no significant difference in tumor outcomes for any dose of IL-2. Indeed, recent studies have called into question whether giving high-dose IL-2 with adoptive T-cell therapy is an optimal approach (Cho et al., 2012).

7. Discussion and conclusions

In summary, a model has been developed to quantitatively assess how the adaptive immune system affects response to anti-tumor chemotherapy or chemoimmunotherapy. While parameter values could not be determined for specific tumors or patients due to the paucity of experimental data, some general conclusions could be drawn: response to treatment depends strongly on the balance between immunosuppressive and immunostimulatory effects. This balance can shift dramatically depending on both

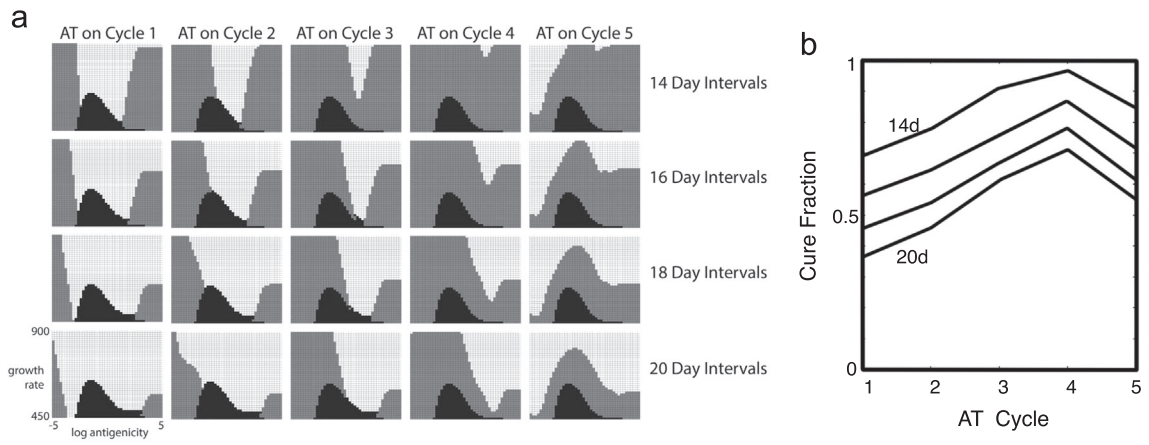

Fig. 9. Effect of adoptive transfer therapy combined with chemotherapy. (a) Each individual image shows the outcome for the range of tumors with log antigenicity between −5 and 5 (horizontal axis) and power law growth coefficient between 450 and 900 (vertical). Black is the region of small steady-state tumors. Gray areas are tumor types that were cured, while white areas are those that escaped therapy. The different outcome charts are for different therapy regimens. The top row of figures are the results for 14-day chemotherapy intervals, increasing by 2 day intervals with each successive row. Each column is the result of applying the adoptive T-cell transfer on a single cycle of the chemotherapy regimen, as labeled along the top of the figure. Poorly antigenic and highly antigenic tumors are cured by the combination therapy. (b) Ratio of the area of the cure region to the area of the total possible cure region (for the full range of growth rate coefficient from 100 to 900), showing that adoptive T-cell transfer is optimized when the cells are administered on the fourth chemotherapy cycle.

innate tumor characteristics such as growth rate and antigenicity, and on the schedule of delivery. The balance can also be shifted in a favorable direction by adding certain immune interventions to chemotherapy.

The model suggests that immune effects occurring naturally (i.e., without any additional immunotherapy) in conjunction with cytotoxic or cytostatic chemotherapy can significantly increase the amount of tumor reduction and control beyond that which can be explained by direct cytotoxicity, but only for certain tumors, characterized by the key parameters of their growth rates and antigenicities. Thus, the model may provide an explanation of what Mitchison (2012) has termed the "proliferation rate paradox," a contradiction in the conventional understanding of how chemotherapy works that was also noted earlier by Craig Thompson (Goodman, 2004). It may also partly explain the benefit of combining cytostatic drugs such as cyclophosphamide with cytotoxic chemotherapy drugs, as both can give the immune system a short-term advantage.

Model predictions indicate the existence of an optimal number of fractions that a total dose of chemotherapy should be divided into, purely based on considerations of tumor-immune interactions. Decreasing the time between chemotherapy cycles is also predicted to improve antitumor immunity. Clinical trials have already shown an advantage to "dose-dense" therapy (i.e., minimizing the interval between chemotherapy cycles), and a recent study by Chang et al. (2012) found that dose-dense therapy reduced immunosuppression and increased effector-T-cell antitumor responses (as evidenced by the surrogate measures of IL-2 and interferon-γ secretion) when compared to a maximum-tolerated-dose regimen in a mouse model. While benefits of dose-dense therapy have been previously rationalized solely in terms of tumor growth kinetics (Simon and Norton, 2006) the present model provides an alternative explanatory mechanism, and also introduces the idea that not only the time between cycles but also the total number of cycles (for a fixed total dose) can affect outcome.

Given the finding that immune effects can contribute significantly to the response from chemotherapy as monotherapy, it is logical to attempt to combine these drugs with other treatments designed specifically to enhance antitumor immunity. The present model shows that not all such immunotherapies that intuitively would be expected to enhance the response to chemotherapy are in fact beneficial in all cases; in fact, some have minimal effect even in the best scenario. Any stimulation of the adaptive immune system will boost both cytotoxic and regulatory T cells. Since these two cell populations have different kinetics of cell proliferation and death, and since they respond differently to certain cytokines and therapies, there are windows of opportunity to simultaneously maximize both the removal of Tregs and the tumor-killing of effector cells. IL-2 therapy is found to be minimally effective because it cannot selectively increase effector T-cell proliferation without also increasing Treg expansion and thus immunosuppression. Adoptive T-cell therapy bypasses this undesirable side effect of Treg expansion and thus is predicted to be more effective, consistent with clinical findings. Dendritic cell vaccination, while having some stimulatory effect on Tregs, promotes effector cell expansion more, and thus, overall, expands the region of tumor control significantly, except for high-antigenicity, high-growth-rate tumors where immunosuppressive effects overwhelm the benefit from the increased dendritic cell population. Treg ablation by an agent such as denileukin diftitox shifts the balance away from immunosuppression in all cases except low-antigenicity tumors where there are not enough effector cells to attack the tumor regardless of the elimination of immunosuppression. While TGF-β blockade, in common with Treg ablation, reduces immunosuppression, it is relatively ineffective because the Tregs remain the more important source of immunosuppression. The model predictions for relative effectiveness of these various forms of chemoimmunotherapy were found to be qualitatively consistent with clinical findings.

Several previous theoretical studies have also examined the role of immune effects in chemotherapy and chemoimmunotherapy, and the implications for optimization of regimen scheduling and dosing. de Pillis et al. (2007) considered only two immune cell populations, the CD8+ effector cells at the tumor site, and the circulating lymphocytes. The latter were used primarily to implement a cost function for optimization, that is, to weigh host toxicity against tumor cell kill. This model did not include immunosuppressive effects or Tregs, and thus the beneficial reduction of the Treg population was not accounted for along with the reduction in effector T cells. Several studies by Leon et al. (2007a,b) incorporated Tregs as well as antigen-presenting cells (which correspond to dendritic cells in the present model). These studies considered separate immune cell populations at the tumor and in the lymph nodes, but then assumed that the tumor and lymph node populations were in equilibrium, making them de

facto single populations. Dendritic cell vaccination, non-specific T cell depletion, and incomplete surgery were modeled, but chemotherapy and chemoimmunotherapy were not considered. The studies by Leon et al. differ from the present model in their use of an exponential growth law for the tumor; a large body of evidence suggests that this growth model does not describe in vivo tumors well over their entire lifetime, although it may be a reasonable approximation for a short enough interval of time.

The model presented in this study has several limitations. The innate immune system was not included, even though it can be an important part of the host anti-tumor response. Another significant source of tumor-induced immunosuppression, the myeloid-derived suppressor cells, was not included. Host toxicity was not modeled; thus it is unknown whether all the combination chemoimmunotherapy regimens simulated are clinically feasible or would give unacceptable side effects. While parameter values were taken whenever possible from human breast cancer studies, in some cases they could only be estimated for other cancer types, or for rodent models, or from in vitro studies. Reasonable assumptions were made about fractional kill from chemotherapy, and the duration of time over which direct chemotherapy-induced cytotoxicity occurred, but these would need to be fine-tuned for specific drugs and tumor types. For immune cells and cytokines, a single body compartment was assumed: cytokine concentrations are in the plasma, and assumed to equilibrate with the tumor; T cell populations are in the tumor compartment and lymphatic periphery. In actuality, it is quite possible that concentrations of cytokines and immune cells differ between the plasma, tumor, and lymph node compartments. Spatially distributed models could capture this, but would require more parameters than the present model uses; moreover, measurements of the values of these parameters might not be available in the literature. Furthermore, while the tumor and lymph node compartments were assumed well-mixed here, spatial gradients are likely within the tumor, and cell population numbers likely differ when going from draining lymph nodes to lymph nodes progressively more distant from the tumor.

Tumor antigenicity was assumed constant over time in the present model, as were parameters associated with the adaptive immune response. In actuality there is experimental evidence for a process sometimes referred to as “immunoediting” (Reiman et al., 2007) whereby the tumor evolves over time to become less responsive to the immune system (von Boehmer et al., 2013; Kottke et al., 2013). This can encompass clonal selection under immune pressure, changes in tumor antigen expression, or tumor-induced corruption of some parts of the immune system to cause it to promote rather than hinder progression. The present model does not include such effects, although previous modeling studies have found them to be significant (d'Onofrio and Ciancio, 2011; Al-Tameemi et al., 2012).

The criterion for tumor removal adopted in this study was a cell number less than 1, as all cell numbers are continuous variables. Given the evidence that not all tumor cells are capable of clonal expansion, it may be that a cell number larger than 1 would be more appropriate; such a threshold has been termed the “cure volume” (Bhardwaj et al., 2007) and could perhaps be estimated from minimal sizes of tumor implants necessary to establish a tumor in mouse models. The study of Caravagna et al. (2010), which used stochastic differential equations to model variability of the immune response, demonstrated that stochastic effects can alter the region of tumor control compared to a deterministic model. Changing the magnitude of random fluctuations would be expected to have a similar effect to changing the threshold “cure volume,” because as fluctuations increase, the likelihood of reaching the cure volume at some point in time increases. Therefore, introducing stochasticity would likely increase the cure region in parameter space.

As mentioned in the section on parameter estimation, another possible source of model error is that the recovery time scales for the T-cell subpopulations were obtained from rodent studies. However, for there to be a benefit from temporary depletion of T-cell subpopulations, all that is required is that the time scales for depletion and recovery are different enough that a window of time exists where the E:R ratio (effector T cell-to-Treg ratio) is more favorable than it was before treatment. Periods of time when the E:R ratio is unfavorable do not offset this outcome because no cell killing occurs during those times. The effect of the E:R ratio is nonlinear, with small values corresponding to virtually no cell kill regardless of how small they are. In view of experimental studies (Ghiringhelli et al., 2004; Pircher et al., 2014) which clearly show different time courses of nadir and recovery for Tregs and effector (or CD4) cells, there is evidence that a window with a more favorable E:R ratio exists regardless of whether the rodent estimates for the T-cell population kinetics are close to human values. Additionally, comparison of the Pircher et al. (2014) data with Lutsiak et al. (2005) suggests little difference in these time scales between rodent and human.

Further, it should be noted that while the above results and discussions for chemoimmunotherapy have focused on how the tumor control region is expanded with the combination of the two therapies, another likely important benefit is the prolongation of survival. This could be further explored with the model, but would probably require tailoring it to specific drugs and tumor types.

The immunological “side-effects” of chemotherapy are very complex, and only certain aspects were explored in this study. Much evidence suggests that chemotherapy is a form of immunotherapy in its own right (in addition to its direct cytotoxic effects) (Zitvogel et al., 2008). However, not all studies show a positive immune effect from chemotherapy. For example, Bandyopadhyay et al. (2010) found that doxorubicin activated TGF-β, and offered this as an explanation for why adding a TGF-β inhibitor improved results from this drug. Such effects were not included in the present study.

In summary, the present model gives insight into the interplay between chemotherapy or chemoimmunotherapy and the adaptive immune system and tumor characteristics, and how these complex nonlinear interactions affect response. It provides a possible answer to the question of how chemotherapy (as monotherapy) actually works, since the traditionally accepted explanation of direct cytotoxicity on rapidly dividing cells is not satisfactory. The model can explain why some immunotherapeutic interventions are only minimally effective when combined with chemotherapy, while others are quite effective, at least for some tumor types. Most importantly, it suggests that both the tumor characteristics, which vary from one patient to another, and the schedule of administration can have a profound impact on outcomes from chemoimmunotherapy. Depending on the tumor characteristics, even the optimal type of chemoimmunotherapy (e.g., dendritic cell vaccine vs. adoptive T-cell transfer) can change significantly. Thus, the opportunities for personalized medicine in chemoimmunotherapy appear to be very promising.

Acknowledgments

A.G. is a Wolfson Royal Society Merit Holder and acknowledges support from a Reintegration Grant under EC Framework VII.

Appendix A. Supplementary data

Supplementary data associated with this paper can be found in the online version at http://dx.doi.org/10.1016/j.jtbi.2015.06.009.

References

Abbas, Abul K., Lichtman, Andrew H.H., Pillai, Shiv, 2012. Basic Immunology: Functions and Disorders of the Immune System. Elsevier Health Sciences, Philadelphia, PA.

Abe, Ikuo, Suzuki, Maroh, Hori, Katsuyoshi, Saito, Sachiko, Sato, Haruo, 1985. Some aspects of size-dependent differential drug response in primary and metastatic tumors. Cancer Metastasis Rev. 4 (1), 27–39.

Akiyama, Yasuto, Oshita, Chie, Kume, Akiko, Iizuka, Akira, Miyata, Haruo, Komiyama, Masaru, Ashizawa, Tadashi, Yagoto, Mika, Abe, Yoshiaki, Mitsuya, Koichi, et al., 2012. α-type-1 polarized dendritic cell-based vaccination in recurrent high-grade glioma: a phase I clinical trial. BMC Cancer 12 (1), 623.

Al-Tameemi, Mohannad, Chaplain, Mark, d'Onofrio, Alberto, 2012. Evasion of tumours from the control of the immune system: consequences of brief encounters. Biol. Direct 7 (1), 31.

Bandyopadhyay, Abhik, Wang, Long, Agyin, Joseph, Tang, Yuping, Tang, Yuping, Lin, Shu, Yeh, I-Tien, De, Keya, Sun, Lu-Zhe, 2010. Doxorubicin in combination with a small TGFβ inhibitor: a potential novel therapy for metastatic breast cancer in mouse models. PLoS One 5 (4), e10365.

Barnett, B., Kryczek, I., Cheng, P., Zou, W., Curiel, T.J., 2005. Regulatory T cells in ovarian cancer: biology and therapeutic potential. Am. J. Reprod. Immunol. 54 (6), 369–377.

Baxevanis, Constantin N., Perez, Sonia A., Papamichail, Michael, 2009. Combinatorial treatments including vaccines, chemotherapy and monoclonal antibodies for cancer therapy. Cancer Immunol. Immunother. 58 (3), 317–324.

Bergmann-Leitner, E.S., Abrams, S.I., 2001. Treatment of human colon carcinoma cell lines with anti-neoplastic agents enhances their lytic sensitivity to antigen-specific CD8$^+$ cytotoxic T lymphocytes. Cancer Immunol. Immunother. 50 (9), 445–455.

Bhardwaj, Sushil, Duggan, David, Kirshner, Jeffrey J., Woolf, Susan, Holland, James F., Berry, Donald A., Norton, Larry, Henderson, I. Craig, 2007. An intensive sequenced adjuvant chemotherapy regimen for breast cancer, a pilot study of the cancer and leukemia group B. Cancer Ther. 5, 117–124.

Bhola, Neil E., Balko, Justin M., Dugger, Teresa C., Kuba, María Gabriela, Sánchez, Violeta, Sanders, Melinda, Stanford, Jamie, Cook, Rebecca S., Arteaga, Carlos L., 2013. Tgf-β inhibition enhances chemotherapy action against triple-negative breast cancer. J. Clin. Investig. 123 (3), 1348.

Bosl, George J., Geller, Nancy L., Cirrincione, Constance, Vogelzang, Nicholas J., Kennedy, B.J., Whitmore, Willet F., Vugrin, Davor, Scher, Howard, Nisselbaum, Jerome, Golbery, Robert B., 1983. Multivariate analysis of prognostic variables in patients with metastatic testicular cancer. Cancer Res. 43 (7), 3403–3407.

Bouchard, Edward W., Falen, Steven, Molina, Paul L., 2002. Lung cancer: a radiologic overview. Appl. Radiol. 31 (8), 7–9.

Brossart, P., Wirths, S., Stuhler, G., Reichardt, V.L., Kanz, L., Brugger, W., 2000. Induction of cytotoxic T-lymphocyte responses in vivo after vaccinations with peptide-pulsed dendritic cells. Blood 96 (9), 3102.

Bubeník, Jan, 2004. MHC class I down-regulation: tumour escape from immune surveillance? (review). Int. J. Oncol. 25 (2), 487–491.

Caravagna, Giulio, d'Onofrio, Alberto, Milazzo, Paolo, Barbuti, Roberto, 2010. Tumour suppression by immune system through stochastic oscillations. J. Theor. Biol. 265 (3), 336–345.

Carlisle, Diane L., Devereux, Wendy L., Hacker, Amy, Woster, Patrick M., Casero, Robert A., 2002. Growth status significantly affects the response of human lung cancer cells to antitumor polyamine-analogue exposure. Clin. Cancer Res. 8 (8), 2684–2689.

Casati, Anna, Zimmermann, Valérie S., Benigni, Fabio, Bertilaccio, Maria T.S., Bellone, Matteo, Mondino, Anna, 2005. The immunogenicity of dendritic cell-based vaccines is not hampered by doxorubicin and melphalan administration. J. Immunol. 174 (6), 3317–3325.

Castillo, Sandra D., Matheu, Ander, Mariani, Niccolo, Carretero, Julian, Lopez-Rios, Fernando, Lovell-Badge, Robin, Sanchez-Cespedes, Montse, 2012. Novel transcriptional targets of the SRY-HMG box transcription factor SOX4 link its expression to the development of small cell lung cancer. Cancer Res. 72 (1), 176–186.

Chang, Li-Yuan, Lin, Yung-Chang, Mahalingam, Jayashri, Huang, Ching-Tai, Chen, Ten-Wen, Kang, Chiao-Wen, Peng, Hui-Min, Chu, Yu-Yi, Chiang, Jy-Ming, Dutta, Avijit, et al., 2012. Tumor-derived chemokine CCL5 enhances TGF-β-mediated killing of CD8+ T cells in colon cancer by T-regulatory cells. Cancer Res. 72 (5), 1092–1102.

Cho, Hyun-il, Reyes-Vargas, Eduardo, Delgado, Julio C., Celis, Esteban, 2012. A potent vaccination strategy that circumvents lymphodepletion for effective antitumor adoptive T-cell therapy. Cancer Res. 72 (8), 1986–1995.

Chu, Christina S., Boyer, Jean, Schullery, Daniel S., Gimotty, Phyllis A., Gamerman, Victoria, Bender, James, Levine, Bruce L., Coukos, George, Rubin, Stephen C., Morgan, Mark A., et al., 2012. Phase I/II randomized trial of dendritic cell vaccination with or without cyclophosphamide for consolidation therapy of advanced ovarian cancer in first or second remission. Cancer Immunol. Immunother. 61 (5), 629–641.

Citron, M.L., Berry, D.A., Cirrincione, C., Hudis, C., Winer, E.P., Gradishar, W.J., Davidson, N.E., Martino, S., Livingston, R., Ingle, J.N., et al., 2003. Randomized trial of dose-dense versus conventionally scheduled and sequential versus concurrent combination chemotherapy as postoperative adjuvant treatment of node-positive primary breast cancer: first report of Intergroup Trial C9741/Cancer and Leukemia Group B Trial 9741. J. Clin. Oncol. 21 (11), 2226.

Curiel, T.J., 2007. Tregs and rethinking cancer immunotherapy. J. Clin. Invest. 117 (5), 1167–1174.

d'Onofrio, Alberto, 2010. Bounded-noise-induced transitions in a tumor-immune system interplay. Phys. Rev. E 81 (2), 021923.

d'Onofrio, Alberto, Ciancio, Armando, 2011. Simple biophysical model of tumor evasion from immune system control. Phys. Rev. E 84 (3), 031910.

de Pillis, L.G., Radunskaya, A.E., Wiseman, C.L., 2005. A validated mathematical model of cell-mediated immune response to tumor growth. Cancer Res. 65 (17), 7950.

de Pillis, Lisette G., Fister, K. Renee, Gu, Weiqing, Collins, Craig, Daub, Michael, Gross David, Moore, James, Preskill, Ben, 2007. Seeking bang–bang solutions of mixed immuno-chemotherapy of tumors. Electron. J. Differ. Equ. 2007(171), 1–24.

Dudley, M.E., Wunderlich, J.R., Robbins, P.F., Yang, J.C., Hwu, P., Schwartzentruber, D. J., Topalian, S.L., Sherry, R., Restifo, N.P., Hubicki, A.M., et al., 2002. Cancer regression and autoimmunity in patients after clonal repopulation with anti-tumor lymphocytes. Science 298 (5594), 850.

Emens, LA., Machiels, J.P., Reilly, R.T., Jaffee, E.M., 2001. Chemotherapy: friend or foe to cancer vaccines?. Curr. Opin. Mol. Ther. 3 (1), 77.

Ercolini, A.M., Ladle, B.H., Manning, E.A., Pfannenstiel, L.W., Armstrong, T.D., Machiels, J.P., Bieler, J.G., Emens, L.A., Reilly, R.T., Jaffee, E.M., 2005. Recruitment of latent pools of high-avidity CD8$^+$ T cells to the antitumor immune response. J. Exp. Med. 201, 1591–1602.

Foss, F., 2006. Clinical experience with denileukin diftitox (ONTAK). Semin. Oncol. 33(1 Suppl. 3), S11–S116.

Gameiro, Sofia R., Caballero, Jorge A., Higgins, Jack P., Apelian, David, Hodge, James W., 2011. Exploitation of differential homeostatic proliferation of t-cell subsets following chemotherapy to enhance the efficacy of vaccine-mediated antitumor responses. Cancer Immunol. Immunother. 60 (9), 1227–1242.

Gardner, Renee V., Lerner, Charles, Astle, Clinton M., Harrison, David E., 1993. Assessing permanent damage to primitive hematopoietic stem cells after chemotherapy using the competitive repopulation assay. Cancer Chemother. Pharmacol. 32 (6), 450–454.

Geara, Fady, Le Bourgeois, Jean Paul, Piedbois, Pascal, Pavlovitch, Jean Marc, Mazeron, Jean Jacques, 1991. Radiotherapy in the management of cutaneous epidemic Kaposi's sarcoma. Int. J. Radiat. Oncol. Biol. Phys. 21 (6), 1517–1522.

Gerber, David E., 2008. Targeted therapies: a new generation of cancer treatments. Am. Fam. Physician 77 (3), 311–319.

Ghiringhelli, François, Larmonier, Nicolas, Schmitt, Elise, Parcellier, Arnaud, Cathelin, Dominique, Garrido, Carmen, Chauffert, Bruno, Solary, Eric, Bonnotte, Bernard, Martin, François, 2004. Cd4+ CD25+ regulatory T cells suppress tumor immunity but are sensitive to cyclophosphamide which allows immunotherapy of established tumors to be curative. Eur. J. Immunol. 34 (2), 336–344.

Gong, Xing, Schwartz, Philip H., Linskey, Mark E., Bota, Daniela A., 2011. Neural stem/progenitors and glioma stem-like cells have differential sensitivity to chemotherapy. Neurology 76 (13), 1126–1134.

Goodman, L., 2004. The kiss of death. J. Clin. Invest. 113 (12), 1662.

Jensen, Ryan, Glazer, Peter M., 2004. Cell-interdependent cisplatin killing by Ku/DNA-dependent protein kinase signaling transduced through gap junctions. Proc. Natl. Acad. Sci. USA 101 (16), 6134–6139.

Josefowicz, Steven Z., Lu, Li-Fan, Rudensky, Alexander Y., 2012. Regulatory T cells: mechanisms of differentiation and function. Annu. Rev. Immunol. 30, 531–564.

June, C.H., 2007. Adoptive T cell therapy for cancer in the clinic. J. Clin. Investig. 117 (6), 1466–1476.

Kerbel, Robert S., Kamen, Barton A., 2004. The anti-angiogenic basis of metronomic chemotherapy. Nat. Rev. Cancer 4 (6), 423–436.

Kirschner, D., Panetta, J.C., 1998. Modeling immunotherapy of the tumor–immune interaction. J. Math. Biol. 37 (3), 235–252.

Kottke, Timothy, Boisgerault, Nicolas, Diaz, Rosa Maria, Donnelly, Oliver, Rommelfanger-Konkol, Diana, Pulido, Jose, Thompson, Jill, Mukhopadhyay, Debabrata, Kaspar, Roger, Coffey, Matt, et al., 2013. Detecting and targeting tumor relapse by its resistance to innate effectors at early recurrence. Nat. Med. 19 (12), 1625–1631.

Laino, Charlene, 2013. Neoadjuvant chemotherapy shown to benefit many younger women with breast cancer. Oncol. Times 35, 25.

Leon, K., Garcia, K., Carneiro, J., Lage, A., 2007a. How regulatory CD25$^+$ CD4$^+$ T cells impinge on tumor immunobiology? On the existence of two alternative dynamical classes of tumors. J. Theor. Biol. 247 (1), 122–137.

Leon, Kalet, Garcia, Karina, Carneiro, Jorge, Lage, Agustin, 2007b. How regulatory CD25+ CD4+ T cells impinge on tumor immunobiology: the differential response of tumors to therapies. J. Immunol. 179 (9), 5659–5668.

Levasseur, L.M., Slocum, H.K., Rustum, Y.M., Greco, W.R., 1998. Modeling of the time-dependency of in vitro drug cytotoxicity and resistance. Cancer Res. 58 (24), 5749.

Liseth, Knut, Ersvær, Elisabeth, Hervig, Tor, Bruserud, Øystein, 2010. Combination of intensive chemotherapy and anticancer vaccines in the treatment of human malignancies: the hematological experience. J. Biomed. Biotechnol. 692097. http://dx.doi.org/10.1155/2010/692097. (Epub 2010 Jun 2).

Liu, V.C., Wong, L.Y., Jang, T., Shah, A.H., Park, I., Yang, X., Zhang, Q., Lonning, S., Teicher, B.A., Lee, C., 2007. Tumor evasion of the immune system by converting CD4$^+$ CD25$^-$ T cells into CD4$^+$ CD25$^+$ T regulatory cells: role of tumor-derived TGF-β. J. Immunol. 178 (5), 2883.

Liu, Liang, Zhu, Xiao-Dong, Wang, Wen-Quan, Shen, Yuan, Qin, Yi, Sun, Hui-Chuan, Tang, Zhao-You, 2010. Activation of β-catenin by hypoxia in hepatocellular carcinoma contributes to enhanced metastatic potential and poor prognosis. Clin. Cancer Res. 16 (10), 2740–2750.

Lutsiak, M.E., Semnani, R.T., de Pascalis, R., Kashmiri, S.V., Schlom, J., Sabzevari, H., 2005. Inhibition of CD4$^+$ CD25$^+$ T regulatory cell function implicated in

enhanced immune response by low-dose cyclophosphamide. Blood 105, 2862–2868.
Manthey, Carl L., Perera, Pin-Yu, Salkowski, Cindy A., Vogel, Stefanie N., 1994. Taxol provides a second signal for murine macrophage tumoricidal activity. J. Immunol. 152 (2), 825–831.
Matsui, Ken, Wang, Zheng, McCarthy, Timothy J., Allen, Paul M., Reichert, David E., 2004. Quantitation and visualization of tumor-specific T cells in the secondary lymphoid organs during and after tumor elimination by pet. Nucl. Med. Biol. 31 (8), 1021–1031.
Matsushita, Hirokazu, Vesely, Matthew D., Koboldt, Daniel C., Rickert, Charles G., Uppaluri, Ravindra, Magrini, Vincent J., Arthur, Cora D., White, J. Michael, Chen, Yee-Shiuan, Shea, Lauren K., et al., 2012. Cancer exome analysis reveals a T-cell-dependent mechanism of cancer immunoediting. Nature 482 (7385), 400–404.
McCoy, M.J., Lake, R.A., van der Most, R.G., Dick, I.M., Nowak, A.K., 2012. Post-chemotherapy t-cell recovery is a marker of improved survival in patients with advanced thoracic malignancies. Br. J. Cancer 107 (7), 1107–11115. http//:dx.doi.org/10.1038/bjc.2012.362.
McKinnell, Robert G., 1998. The Biological Basis of Cancer. Cambridge University Press, Cambridge, UK.
Minchinton, Andrew I., Tannock, Ian F., 2006. Drug penetration in solid tumours. Nat. Rev. Cancer 6 (8), 583–592.
Mitchison, Timothy J., 2012. The proliferation rate paradox in antimitotic chemotherapy. Mol. Biol. Cell 23 (1), 1–6.
Newell, M. Karen, Melamede, Robert, Villalobos-Menuey, Elizabeth, Swartzendruber, Douglas, Trauger, Richard, Camley, Robert E., Crisp, William, 2004. The effects of chemotherapeutics on cellular metabolism and consequent immune recognition. J. Immune Based Ther. Vaccines 2 (1), 3.
Norton, L., 2001. Theoretical concepts and the emerging role of taxanes in adjuvant therapy. Oncologist, 6 (Supplement 3), 30.
Norton, Larry, Simon, Richard, 1986. The Norton Simon hypothesis revisited. Cancer Treat. Reports 70 (1), 163–169.
Palucka, Karolina, Banchereau, Jacques, 2012. Cancer immunotherapy via dendritic cells. Nat. Rev. Cancer 12 (4), 265–277.
Pfannenstiel, Lukas W., Lam, Samuel S.K., Emens, Leisha A., Jaffee, Elizabeth M., Armstrong, Todd D., 2010. Paclitaxel enhances early dendritic cell maturation and function through TLR4 signaling in mice. Cellular Immunol. 263 (1), 79–87.
Pircher, Andreas, Gamerith, Gabriele, Amann, Arno, Reinold, Susanne, Popper, Helmut, Gächter, Anneliese, Pall, Georg, Wöll, Ewald, Jamnig, Herbert, Gastl, Günther, et al., 2014. Neoadjuvant chemo-immunotherapy modifies CD4+ CD25+ regulatory T cells (Treg) in non-small cell lung cancer (NSCLC) patients. Lung Cancer 85 (1), 81–87.
Pries, Axel R., Cornelissen, Annemiek J.M., Sloot, Anoek A., Hinkeldey, Marlene, Dreher, Matthew R., Höpfner, Michael, Dewhirst, Mark W., Secomb, Timothy W., 2009. Structural adaptation and heterogeneity of normal and tumor microvascular networks. PLoS Comput. Biol. 5 (5), e1000394.
Rasku, M.A., Clem, A.L., Telang, S., Taft, B., Gettings, K., Gragg, H., Cramer, D., Lear, S. C., McMasters, K.M., Miller, D.M., et al., 2008. Transient T cell depletion causes regression of melanoma metastases. J. Transl. Med. 6 (1), 12.
Reiman, Jennifer M., Kmieciak, Maciej, Manjili, Masoud H., Knutson, Keith L., 2007. Tumor immunoediting and immunosculpting pathways to cancer progression. Semin. Cancer Biol. 17 (4), 275–287.
Robertson-Tessi, Mark, El-Kareh, Ardith, Goriely, Alain, 2012. A mathematical model of tumor–immune interactions. J. Theor. Biol. 294, 56–73.
Rosenberg, S.A., Yannelli, J.R., Yang, J.C., Topalian, S.L., Schwartzentruber, D.J., Weber, J.S., Parkinson, D.R., Seipp, C.A., Einhorn, J.H., White, D.E., 1994. Treatment of patients with metastatic melanoma with autologous tumor-infiltrating lymphocytes and interleukin-2. J. Natl. Cancer Inst. 86 (15), 1159.
Sahani, Dushyant V., Kalva, Sanjeeva P., 2004. Imaging the liver. The Oncologist 9 (4), 385–397.
Sanga, S., Sinek, J.P., Frieboes, H.B., Ferrari, M., Fruehauf, J.P., Cristini, V., 2006. Mathematical modeling of cancer progression and response to chemotherapy. Exp. Rev. Anticancer Ther. 6 (10), 1361–1376.
Schlom, Jeffrey, 2012. Therapeutic cancer vaccines: current status and moving forward. J. Natl. Cancer Inst. 104 (8), 599–613.
Schmitt, C.A., 2007. Cellular senescence and cancer treatment. Biochim. Biophys. Acta Rev. Cancer 1775 (1), 5–20.
Simon, Richard, Norton, Larry, 2006. The Norton Simon hypothesis: designing more effective and less toxic chemotherapeutic regimens. Nature Clin. Pract. Oncol. 3 (8), 406–407.
Smith, R.A., Cokkinides, V., von Eschenbach A.C., Levin, B., Cohen, C., Runowicz, C.D., Sener, S., Saslow, D., Eyre, H.J., 2002. American Cancer Society guidelines for the early detection of cancer. Cancer J. Clin. 52 (1), 8.
Suzuki, E., Kapoor, V., Cheung, H.K., Ling, L.E., DeLong, P.A., Kaiser, L.R., Albelda, S.M., 2004. Soluble type II transforming growth factor-β receptor inhibits established murine malignant mesothelioma tumor growth by augmenting host antitumor immunity. Clin. Cancer Res. 10 (17), 5907.
Tay, D.L., Bhathal, P.S., Fox, R.M., 1991a. Quantitation of G0 and G1 phase cells in primary carcinomas. antibody to M1 subunit of ribonucleotide reductase shows G1 phase restriction point block. J. Clin. Invest. 87 (2), 519.
Trédan, Olivier, Galmarini, Carlos M., Patel, Krupa, Tannock, Ian F., 2007. Drug resistance and the solid tumor microenvironment. J. Natl. Cancer Inst. 99 (19), 1441–1454.
Uhl, M., Aulwurm, S., Wischhusen, J., Weiler, M., Ma, J.Y., Almirez, R., Mangadu, R., Liu, Y.W., Platten, M., Herrlinger, U., et al., 2004. SD-208, a novel transforming growth factor β receptor I kinase inhibitor, inhibits growth and invasiveness and enhances immunogenicity of murine and human glioma cells in vitro and in vivo. Cancer Res. 64 (21), 7954.
Vo, Thanh-Trang, Ryan, Jeremy, Carrasco, Ruben, Neuberg, Donna, Rossi, Derrick J., Stone, Richard M., DeAngelo, Daniel J., Frattini, Mark G., Letai, Anthony, 2012. Relative mitochondrial priming of myeloblasts and normal HSCs determines chemotherapeutic success in AML. Cell 151 (2), 344–355.
von Boehmer, Lotta, Mattle, Muriel, Bode, Peter, Landshammer, Alexandro, Schäfer, Carolin, Nuber, Natko, Ritter, Gerd, Old, Lloyd, Moch, Holger, Schäfer, Niklaus, 2013. Ny-eso-1-specific immunological pressure and escape in a patient with metastatic melanoma. Cancer Immun. 13.
Weir, Genevieve M., Liwski, Robert S., Mansour, Marc, 2011. Immune modulation by chemotherapy or immunotherapy to enhance cancer vaccines. Cancers 3 (3), 3114–3142.
Wheeler, Christopher J., Das, Asha, Liu, Gentao, John, S. Yu, Black, Keith L., 2004. Clinical responsiveness of glioblastoma multiforme to chemotherapy after vaccination. Clin. Cancer Res. 10 (16), 5316–5326.
Wiltshaw, Eve, 1979. Cisplatin in the treatment of cancer. Plat. Metals Rev. 23, 90–98.
Zeman, E.M., 2000. Biologic basis of radiation oncology. In: Gunderson, L.L., Tepper, J.E. (Eds.), Clinical Radiation Oncology, pp. 1–46.
Zitvogel, L., Apetoh, L., Ghiringhelli, F., Kroemer, G., 2008. Immunological aspects of cancer chemotherapy. Nat. Rev. Immunol. 8 (1), 59–73.